DIGITAL SIMULATION OF NONSTATIONARY RANDOM PROCESSES AND ITS APPLICATIONS†

By

HIROSHI ISHIKAWA*, HIDEHIKO MITSUMA**
and MASANOBU SHINOZUKA***

ABSTRACT

The purpose of the present study is to introduce the data-based nonstationary random process model and to indicate its potential applications especially in engineering, particularly in those cases where efficient generations of its sample functions are needed for the purpose of Monte Carlo and other investigations. The nonstationary process model to be developed is called "data-based" since it is constructed primarily on the basis of the observed record. In fact, the model can be written in the form of the inversion of the Fourier transform of the original record (the first kind) or of its symmetric-periodic extension (the second kind) with randomly shifted phase angles. Its construction is a straightforward task requiring only the Fourier transform of the original

---

† This work has been accomplished during the first author's stay at Columbia University, New York, U.S.A., as a Senior Research Associate in the Department of Civil Engineering and Engineering Mechanics, for the period March, 1977 through March, 1979.

* Ph.D., Associate Professor of Statistics, Junior College of Commerce, Kagawa University, Saiwai-cho, Takamatsu-shi 760 Japan.

** Ph.D., Chief Engineer, National Space Development Agency, Tokyo, Japan.

*** Ph.D., Renwick Professor of Civil Engineering, Department of Civil Engineering and Engineering Mechanics, Columbia University, New York, N. Y. 10027 U.S.A.

record (or its extension) or equivalently its Hilbert transform. Also, the model lends itself to a tractable implementation of Monte Carlo analyses because of the ease with which its sample functions are generated.

CHAPTER 1 INTRODUCTION

The analysis of structural response to various types of random dynamic loadings has long been of interest to engineers. An elaborate theory has been derived for the spectral analysis of stationary random processes and has applied extensively to engineering problems. An increasing number of attempts have been mabe in recent years to extend the concepts associated with classical spectral analysis to certain cases where nonstationarity is the essential feature of the processes involved. Examples are those nonstationary random processes with the instantaneous spectrum, the double frepuency spectrum, the evolutionary spectrum, the physical spectrum and the locally time averaged spectrum.

It is the purpose of this study to introduce the data-based nonstationary random processes and to indicate their potential applications in engineering, particularly in those cases where efficient generations of their sample functions are needed for the purpose of Monte Carlo and other investigations. The nonstationary processes to be introduced are called "data-based" because they are constructed primarily on the basis of the observed record.[1],[2]

The data-based nonstationary random processes are simple to construct and possess a convenient analytical form for the generation of their sample functions, particularly as compared with other nonstationary random process representation such as those mentioned earlier.

In the following, an effort is made in Chapter 2 to place the data-based nonstationary model in a proper perspective against the technical background involving the nonstationary random process models currently available. In Chapter 3, we construct the model and examine its characteristics in detail. Chapter 4 then provides numerical examples where the model is applied to a number of observed records of practical interest. Finally, Chapter 5 delineates the findings of the present study.

CHAPTER 2 TECHNICAL BACKGROUND

2. 1 Introduction

It is well recognized that the lack of ergodicity is the most significant characteristic of nonstationary random processes in terms of their engineering applications, since it considerably obscures the reliability of the estimates of such key statistical parameters as mean value and autocorrelation function when the number of sample functions is limited to only a few, if not just one. Unfortunately, this smallness of the sample size is usually the case when we wish to apply nonstationary random process theory in the field of structural engineering and engineering mechanics. Indeed, it would be a rare occasion for us to be in possession of a large number of sample functions on which the statistical analysis can be performed to reproduce the ensemble characteristics of, and further to develop the model of, their population nonstationary process. In the present study, however, we are primarily concerned with the method of constructing nonstationary process models but not specifically with estimating the characteristics of statistical parameters. It is pointed out, however, that the nonstationary model to be proposed later in this study has a unique feature in that its construction requires only a straightforward evaluation of the Fourier transform of the observed record and related quantities (hence the name of "data-based" nonstationary random process).[(1),(2)] Thus we are often able to eliminate theoretically awkward and numerically cumbersome efforts for statistical estimation involving sample functions of nonstationary random processes.

Examination of the nonstationary random process models proposed so far indicates that they may be classified into two general categories. One category consists of a class of models that might be termed as time domain models while the other as frequency domain models.

2. 2 Time Domain Models

Although the present study places its emphasis on frequency domain models, the following brief description seems to be appropriate with respect to some typical time domain models either in the form of the filtered Poisson (or shot noise) process[(3),(4)] or in the form derived from the filtered white noise process.

The filtered Poisson or shot noise process model was originally used to simulate some of the physical phenomena observed in the field of electric and electronic engineering and more recently was found to be useful also in the fields of structural engineering and engineering mechanics.[(5),(6)]

In its general form, the filtered Poisson process is written as

$$\boldsymbol{x}(t)=\sum_{n=-\infty}^{\boldsymbol{N}(t)} \boldsymbol{A}_n w(t,\ \boldsymbol{\tau}_n) \tag{2. 1}$$

where $w(t,\ \tau)$ = shape function representing the effect at time t of a signal arriving at time τ and therefore $w(t,\ \tau)=0$ for $t \leqq \tau$, $\boldsymbol{N}(t)$ = Poisson process with arrival times $\cdots\cdots \boldsymbol{\tau}_{-1}<\boldsymbol{\tau}_0<\boldsymbol{\tau}_1 \cdots\cdots$ and $\boldsymbol{A}_n$ = an identically distributed random variable representing the magnitude of the signal arriving at $t=\boldsymbol{\tau}_n$.[(*1)] This process is easy to construct and can be made nonstationary by assuming, for example, that the mean arrival rate of the Poisson process is a function of time.[(3),(5)] Analytical expressions for the mean value, variance, autocorrelation function and characteristic function are

(*1) Throughout the present paper, stochastic quantities shall be boldfaced.

generally available.[3] The probability density and autocorrelation functions can be obtained at least in principle as the inverse Fourier transforms of characteristic and generalized spectral density functions, respectively. Also of practical importance is the fact that the sample functions of this process, whether stationary or nonstationary, can be generated in the time domain by making a direct use of Eq. 2. 1.

The filtered white noise process in the present study refers to the process $\xi(t)$ which satisfies the following equation:

$$L[\xi(t)]=n_0(t) \tag{2. 2}$$

in which $L[\cdot]$=a linear operator and $n_0(t)$=a (stationary) Gaussian white noise with a constant spectral density S_0. The Gaussian assumption coupled with the assumed linearity of the operator in general makes it relatively easy to evaluate the mean value, variance, autocorrelation function, spectral density $S_{\xi\xi}(\omega)$ of the resulting stationary Gaussian process $\xi(t)$. Due to the conceptual simplicity and the analytical familiarity, this model has so far been quite popular among those in the areas of structural engineering and engineering mechanics. In particular, in its application to the earthquake-related research, linear differential operators with constant coefficients are often used for the operator $L[\cdot]$. In this case the frequency response function $H(\omega)$ associated with the operator can easily be evaluated and, as is well known, the mean square spectral density of $\xi(t)$ is given by $S_{\xi\xi}(\omega)=S_0\,|\,H(\omega)\,|^2$. Derivation of the mean value, variance, autocorrelation function, etc. then becomes a straightforward task of algebraic manipulation and evaluation of the integrals involved.

We can now introduce the amplitude modulated nonstationary random process defined as

$$x(t)=g(t)\cdot\xi(t) \tag{2. 3}$$

where $g(t)$ is a deterministic function of time such that it is equal to zero outside of the interval $[0, T_0]$ while it varies slowly within the interval. If the variation of $g(t)$ is much slower than that of the sample functions of the process $\xi(t)$, the spectral content of $\xi(t)$ is expected to prevail in approximation for the process $x(t)$ as well. Again, it is of practical importance to note that the nonstationary random process $x(t)$ can be constructed easily and that its sample functions can be generated directly in the time domain with the aid of Eq. 2. 3. For this purpose, however, we suggest the use of a technique that generates sample functions of $\xi(t)$, a stationary Gaussian process with zero mean in terms of the sum of cosine functions basically involving only the mean square spectral density function. A specific reference will be made to this technique later in this study.

2. 3 Frequency Domain Models

In the present study, those stochastic models are called frequency domain models if they can produce nonstationary random processes and corresponding sample functions which can reproduce the specified nonstationary spectral density. There are, however, a number of definitions of nonstationary spectral density in the literature. Most well known are the generalized spectrum (or double frequency spectrum)[(7)–(10)], the instantaneous spectrum[(11)–(16)], the physical spectrum[(16)], the locally time averaged spectrum[(17)] and the evolutionary spectrum.[(18)–(23)] From the viewpoint of application, particularly in the fields of structural engineering and engineering mechanics, any (nonstationary) spectrum should have the following features: (a) It is physically meaningful, (b) a simple transition from nonstatioinary to stationary spectrum is possible, (c) dealing with a linear system, the input-output relationship can be described in a simple manner in terms of the input and output nonstationary spectra (under the same definition) and the system transfer functoin, (d) it can be obtained by an integral transormation, preferably by the Fourier transformation, from the nonstationary autocorrefation function and finally (e) its estimation on the basis of observed records is not too difficult. Each of the nonstationary spectra listed above satisfies these requirements to a varying degree of success, although none satisfies all the requirements completely. The following observation is in order at this point: These spectra can be used to characterize and sometimes conveniently estimate the nonstationary spectral contents of given time records. However, they are, with the exception of the evolutionary spectrum, not particularly suited for being incorporated into a stochastic model in such a way that the model produces a nonstationary random process characterized by one of these nonstationary spectra and at the same time generates their sample functions with practical ease.

On the basis of the observation above, we examine below the stochastic model that incorporates the evolutionary spectral density.

For this purpose, we first consider the following spectral representation of a stationary random process $x(t)$;

$$x(t)=\int_{-\infty}^{\infty}\exp(i\omega t)\,dF(\omega) \tag{2.4}$$

where $F(\omega)$, called the spectral process, is orthogonal in the sense that the increments $dF(\omega_1)$ and $dF(\omega_2)$ are uncorrelated when $\omega_1 \neq \omega_2$. By employing the orthogonal condition of $F(\omega)$, we can show that the autocorrelation $R_{xx}(\tau)$ of $x(t)$ is

$$R_{xx}(\tau)=\int_{-\infty}^{\infty}\exp(i\omega\tau)\,\mathrm{E}\{\,|\,dF(\omega)\,|^2\} \tag{2.5}$$

Assume that the spectral density function $S_0(\omega)$ exists. Then $\mathrm{E}\{\,|\,dF(\omega)\,|^2\}=S_0(\omega)d\omega$, and Eq. 2.5 reduces to the well-known Wiener-Khintchine relationship. For the case where $x(t)$ is real,

$$x(t)=\int_{0}^{\infty}[\cos\omega t\,dU(\omega)+\sin\omega t\,dV(\omega)] \tag{2.6}$$

where $U(\omega)$ and $V(\omega)$ for any $\omega\geqq 0$ are two mutually orthogonal processes, both real and with orthogonal increments such that

$$E\{dU(\omega)^2\}=E\{dV(\omega)^2\}=S_1(\omega)d\omega \tag{2. 7}$$

Construct now the following process

$$x(t)=\sqrt{2}\sum_{k=1}^{n}\{S_1(\omega_k)\Delta\omega\}^{1/2}\cos(\omega_k t+\Phi_k) \tag{2. 8}$$

where $\omega_k=k\Delta\omega$, $\omega_u=n\Delta\omega$ is the upper cut-off frequency beyond which $S_1(\omega)$ is either actually or approximately zero, and Φ_k's are statistically independent random phases uniformly distributed between $-\pi$ and π. If we define in Eq. 2.6 that

$$\begin{aligned} dU(\omega_k)&=[2S_1(\omega_k)\Delta\omega]^{1/2}\cos\Phi_k \\ dV(\omega_k)&=[2S_1(\omega_k)\Delta\omega]^{1/2}\sin\Phi_k \end{aligned} \tag{2. 9}$$

then all the conditions imposed on $U(\omega)$ and $V(\omega)$ are satisfied, and x(t) in Eq. 2.8 is basically consistent with and approximate to its spectral representation given by Eq. 2.6.

Due to the fact that Φ_k's are statistically independent and uniformly distributed between $-\pi$ and π, the process $x(t)$ in Eq. 2.8 tends to Gaussian with zero mean as $n\to\infty$ by virtue of the central limit theorem. In fact, this process $x(t)$ is the form which has been extensively used,[(24),(25)] together with the FFT (Fast Fourier Transform) technique, to generate sample functions of Gaussian processes with zero mean and given (one-sided) spectral density $S_1(\omega)$.

Eq. 2.6 indicates that a stationary process can be additively "built up" by orthogonal oscillations with random amplitudes. This concept of orthogonal components can be extended to that of the evolutionary process $x(t)$ expressed as

$$x(t)=\int_0^\infty B(t,\ \omega)[\cos\omega t dU(\omega)+\sin\omega t dV(\omega)] \tag{2.10}$$

where $B(t,\ \omega)$ is a real deterministic modulating function characterizing the nonstationarity of the process, and $U(\omega)$ and $V(\omega)$ are the same as defined in Eq. 2.9. By using the orthogonal conditions of $U(\omega)$ and $V(\omega)$, the mean square of $x(t)$ is found to be

$$\mathrm{E}\{x^2(t)\}=\int_0^\infty B^2(t,\ \omega)S_1(\omega)d\omega=\int_0^\infty S_1(t,\ \omega)d\omega \tag{2.11}$$

where $S_1(t,\ \omega)=B^2(t,\ \omega)S_1(\omega)$ is defined as the evolutionary power spectral density function.

With respect to the requirements mentioned earlier which a desirable nonstationary spectral density is supposed to satisfy, we observe that the evolutionary spectrum defined above indeed satisfies some of them completely while others reasonably well: (a) The evolutionary process can be interpreted as a process "built up" by orthogonal oscillations with time-varying random amplitudes, (b) the evolutionary spectrum reduces to the standard mean square spectral density when $B(t,\ \omega)$ becomes independent of time, (c) the input-output relationship is not as simple as in the stationary cases but can be established,[(23),(26)] (d) the relationship between the evolutionary spectrum and the autocorrelation function can also be established[(27)] although it does not result in a form as elegant as the Wiener-Khintchine relationship in the stationary cases, and finally (e) it appears that reasonable estimations of the spectrum on the basis of observed data are possible particularly when $B(t,\ \omega)$ varies slowly with time.[(22)]

Corresponding to Eq. 2. 8, we have

$$x(t)=\sqrt{2}\sum_{k=1}^{n}\{B^2(t,\ \omega_k)S_1(\omega_k)\Delta\omega\}^{1/2}\cos(\omega_k t+\Phi_k) \tag{2.12}$$

which is an approximation to the evolutionary process $x(t)$ in Eq. 2.10 with $dU(\omega)$ and $dV(\omega)$ defined by Eq. 2.9. Eq. 2.12 can be conveniently used to generate sample functions of the evolutionary process[(27),(28)] if $S_1(\omega)$ and $B(t,\ \omega)$ are specified although in this case the FFT technique cannot be utilized.

At the present time, the process $x(t)$ in Eq. 2.10 together with its practical version given in Eq. 2.12 appears to be the most useful nonstationary process model in the frequency domain.

CHAPTER 3 DATA-BASED NONSTATIONARY RANDOM PROCESSES

3.1 General Remarks

Virtually all of the analytical models of nonstationary random processes investigated to date can be classified into one of the categories discussed earlier. Emphasizing the frequency domain models in general and the evolutionary process in particular, however, we find that two major difficulties are associated with these models from the viewpoint of engineering applications. First, these models characterize the nonstationarity in terms of appropriately modified forms of the mean square spectral density. Unfortunately, however, the mean square spectral density is a notion that is not particularly amenable to nonstationary conditions. Second, the intrinsic lack of the ergodicity in the nonstationary process prevents us from reconstructing its probabilistic nature on the basis of a single sample function. Such a reconstruction, if it is to be performed reasonably well, would require a large number of sample functions. This is a requirement which is totally unrealistic in most practical applications in the field of structural engineering. In fact, dealing with earthquake accelerations, wind-induced pressures on structures, dynamic flight loads on spacecraft, etc., we would be fortunate to have a few, if not one, sample functions purported to be extracted from the same population.

In spite of the difficulties indicated above, the need of nonstationary process models for these and other physical phenomena germane to structural engineering has been increasingly recognized as modern engineering analysis and design demand further sophistications. In particular, the nonstationary process models whose sample functions can easily be generated with the aid of a high speed electronic computer, are extremely useful. They can be incorporated in the time and space domain analysis in conjunction with Monte Carlo techniques to obtain such vital information as first passage time distribution, random response of severely nonlinear structures, etc.[25] The frequency and wave number domain analysis is at best awkward for these purposes.

In this chapter, we introduce another frequency domain model that produces the "data-based" nonstationary random processes, derive their basic characteristics and investigate how they can alleviate most, if not all, of the difficulties described above.

3.2 Data-Based Nonstationary Random Processes of the First Kind

3.2.1 Univariate and one-dimensional processes

Let $x_0(t)$ be an observed record of duration T_0. Throughout the present study, we consider that the record begins at $t=0$ and ends at $t=T_0$ and that it is equal to zero outside the domain $[0, T_0]$. Writing $X_0(\omega)$ for the Fourier transform of $x_0(t)$, we obtain the following Fourier transform pair:

$$x_0(t)=1/(2\pi)\int_{-\infty}^{\infty}X_0(\omega)\exp(i\omega t)d\omega \quad (3.1)$$

$$X_0(\omega)=\int_{-\infty}^{\infty}x_0(t)\exp(-i\omega t)dt \quad (3.2)$$

where i is the imaginary unit. The phase angle $\zeta_0(\omega)$ of $X_0(\omega)$ is given, if $\mathrm{Re}[X_0(\omega)]\neq 0$, by

$$\zeta_0(\omega)=-\zeta_0(-\omega)=\arctan\{\mathrm{Im}[X_0(\omega)]/\mathrm{Re}[X_0(\omega)]\} \quad (3.3)$$

while, if $\mathrm{Re}[X_0(\omega)]=0$, it is given by

$$\zeta_0(\omega)=\pm\pi/2+2k\pi \quad (k=0,\pm1,\pm2,\cdots\cdots) \quad (3.4)$$

where $\mathrm{Re}[X_0(\omega)]=\mathrm{Re}[X_0(-\omega)]=$ real part of $X_0(\omega)$ and $\mathrm{Im}[X_0(\omega)]=-\mathrm{Im}[X_0(-\omega)]=$imaginary part. Using the phase angle, $X_0(\omega)$ and $x_0(t)$

can then be expressed as

$$X_0(\omega) = |X_0(\omega)| \exp\ i\zeta_0(\omega) \tag{3. 5}$$

$$x_0(t) = 1/(2\pi)\int_{-\infty}^{\infty} |X_0(\omega)| \exp i\{\omega t + \zeta_0(\omega)\}\, d\omega \tag{3. 6}$$

where $|X_0(\omega)| = |X_0(-\omega)|$ =Fourier (amplitude) spectrum of $x_0(t)$.

Now construct a nonstationary random process $\boldsymbol{x}(t)$ on the basis of the observation $x_0(t)$:

$$\boldsymbol{x}(t) = 1/(2\pi)\int_{-\infty}^{\infty} |X_0(\omega)| \exp i\{\omega t + \zeta_0(\omega) + \boldsymbol{\phi}(\omega)\}\, d\omega \tag{3.7—a}$$

with the sample functions $x^{(k)}(t)$ in the form:

$$x^{(k)}(t) = 1/(2\pi)\int_{-\infty}^{\infty} |X_0(\omega)| \exp i\{\omega t + \zeta_0(\omega) + \phi^{(k)}(\omega)\}\, d\omega \tag{3.7—b}$$

where the most general definition of $\phi^{(k)}(\omega)$ is such that it is a sample function of a random process $\boldsymbol{\phi}(\omega)$ in ω. A comparison between Eq. 3.7—b and Eq. 3.6 indicates that $x^{(k)}(t)$ is obtained from $x_0(t)$ by replacing its phase angle $\zeta_0(\omega)$ by

$$\zeta^{(k)}(\omega) = \zeta_0(\omega) + \phi^{(k)}(\omega) \tag{3. 8}$$

we choose the following form for the function $\boldsymbol{\phi}(\omega)$,

$$\boldsymbol{\phi}(\omega) = \boldsymbol{\Phi} \cdot \mathrm{sgn}\,(\omega) \tag{3. 9}$$

where $\boldsymbol{\Phi}$= a random variable and sgn $(\omega) = -1$ for $\omega<0$, $=0$ for $\omega=0$ and $=1$ for $\omega>0$. The sample function $\phi^{(k)}(\omega)$ is then given by

$$\phi^{(k)}(\omega) = \Phi^{(k)} \cdot \mathrm{sgn}\,(\omega) \tag{3.10}$$

with $\Phi^{(k)}$ indicating a sample value of $\boldsymbol{\Phi}$. The fact that $x^{(k)}(t)$ is a real function requires that $\phi^{(k)}(\omega)$ be odd; thus the use of the sign function sgn(ω).

The Fourier transform of the simulated precess $\boldsymbol{x}(t)$ can then be given as the inverse Fourier transform of Eq. 3. 7—a in the following form:

$$\begin{aligned} \boldsymbol{X}(\omega) &= |X_0(\omega)| \exp i\{\zeta_0(\omega) + \boldsymbol{\phi}(\omega)\} \\ &= X_0(\omega) \exp i\boldsymbol{\phi}(\omega) \end{aligned} \tag{3.11}$$

Throughout the present study, we assume that the random variable Φ distributes in accordance either with the uniform distribution function with the density

$$f_{\Phi}(x)=1/(2a) \qquad \mu-a\leqq x\leqq\mu+a \quad (a>0)$$
$$=0 \qquad \text{otherwise} \tag{3.12}$$

where $\mu=$ expected value and $2a=$ width of distribution, or with the Gaussian distribution with the density

$$f_{\Phi}(x)=1/(\sqrt{2\pi}\sigma)\exp\{-(x-\mu)^2/(2\sigma^2)\} \qquad -\infty<x<\infty \tag{3.13}$$

where $\mu=$ expected value and $\sigma=$ standard deviation.

At this point, the following heuristic observation is noted for theoretical interest: Formally, we have $d\omega=2\pi/T_0$ and $|X_0(\omega)|=\sqrt{2\pi T_0 S_0(\omega)}$ (as $T_0\rightarrow\infty$) for a stationary random process with a mean square spectral density $S_0(\omega)$. Hence, $1/(2\pi)\cdot|X_0(\omega)|d\omega$ in Eq. 3.7—a becomes $\sqrt{(2\pi/T_0)S_0(\omega)}=\sqrt{S_0(\omega)d\omega}$. Assuming that $\phi(\omega)$ is a Gaussian white noise with zero mean for positive ω and that $\phi(\omega)=-\phi(-\omega)$, we can reduce Eq. 3.7—$a$ into

$$x(t)\cong\sqrt{2}\sum_{k=1}^{n}\sqrt{S_1(\omega_k)\Delta\omega}\cos\{\omega_k t+\phi(\omega_k)\} \tag{3.14}$$

where $S_1(\omega)=2S_0(\omega)$ defined for positive $\omega=$one-sided mean square spectral density; $\omega_k=k\Delta\omega$ and $n\Delta\omega=\omega_u=$upper cut-off frequency beyond which $S_1(\omega)$ is either actually or approximately zero.[(29),(30)] Eq. 3.14 is identical to Eq. 2.8 with $\Phi_k=\phi(\omega_k)$ often used to simulate a stationary Gaussian process with mean zero and spectral density function $S_0(\omega)$. In the process of transforming Eq. 3.7—a into Eq. 3.14, $\zeta_0(\omega)$ has been absorbed into $\phi(\omega)$ which is now a white noise. The comparison of Eq. 3.7—a with Eq. 3.14 indicates that the essential difference between these stationary and nonstationary simulations lies in that the function $\phi(\omega)=-\phi(-\omega)$ is a white noise for positive ω in the stationary case while, in the nonstationay simulation, it is a random variable multiplied by the sign function sgn (ω) as shown in Eq. 3.9 (thus its sample value is not a function of ω but a constant for positive ω).

In view of the fact that $\zeta_0(\omega)+\phi(\omega)$ is an odd function of ω with $\phi(\omega)$ defined by Eq. 3.9, we can rewrite $x(t)$ in Eq. 3.7—a as:

$$x(t)=1/\pi\int_0^\infty |X_0(\omega)| \cos\{\omega t+\zeta_0(\omega)+\Phi\}\, d\omega \tag{3.15}$$

or equivalently,

$$x(t)=x_0(t)\cos\Phi-\hat{x}_0(t)\sin\Phi \tag{3.16}$$

where

$$x_0(t)=1/\pi\int_0^\infty |X_0(\omega)| \cos\{\omega t+\zeta_0(\omega)\}\, d\omega \tag{3.17}$$

is obviously the observed record (see Eqs. 3.1 and 3.2) while

$$\hat{x}_0(t)=1/\pi\int_0^\infty |X_0(\omega)| \sin\{\omega t+\zeta_0(\omega)\}\, d\omega \tag{3.18}$$

The process given by Eq.3.16 is referred to as "*data-based nonstationary process of the first kind.*" In this case, the process is obviously univariate and one-dimensional.

We can show that $\hat{x}_0(t)$ defined in Eq. 3.18 is the Hilbert transform of $x_0(t)$:

$$\begin{aligned}\hat{x}_0(t)&=1/\pi\int_{-\infty}^{\infty} x_0(\tau)/(t-\tau)\, d\tau\\ &=x_0(t)*[1/(\pi t)]\end{aligned} \tag{3.19}$$

where the symbol $*$ indicates a convolution integral.

We can also show under these conditions that the Fourier transform $\hat{X}_0(\omega)$ of $\hat{x}_0(t)$ is given in terms of the Fourier transform $X_0(\omega)$ of $x_0(t)$ as (*2)

$$\hat{X}_0(\omega)=-i\ \mathrm{sgn}(\omega)X_0(\omega) \tag{3.20}$$

(*2) $|X_0(\omega)|$ is even, while $\sin\{\omega t+\zeta_0(\omega)\}$ is odd with respect to ω. Hence, Eq. 3. 18 can be rewritten in the following form:

$$\begin{aligned}\hat{x}_0(t)&=\frac{1}{\pi}\int_0^\infty |X_0(\omega)| \sin\{\omega t+\zeta_0(\omega)\}d\omega\\ &=\frac{1}{2\pi i}\int_{-\infty}^{\infty} |X_0(\omega)|\ \mathrm{sgn}(\omega)\exp i\{\omega t+\zeta_0(\omega)\}d\omega\end{aligned}$$

From the definition of $\hat{x}_0(t)$ given by Eq. 3.19, it follows that, al-

$$=\frac{1}{2\pi}\int_{-\infty}^{\infty}\{-i\,\mathrm{sgn}(\omega)X_0(\omega)\}\exp i\omega t\;d\omega$$

The last expressin of the right-hand side of the above equation shows us that the Fourier transform of $\hat{x}_0(t)$ should be in the form of Eq. 3. 20, that is,

$$\hat{X}_0(\omega)=-i\,\mathrm{sgn}(\omega)X_0(\omega)$$

Further, as is well known, time convolution theorem states that the Fourier transform of the convolution of two functions equals the product of the Fourier transforms of these two functions. Therefore if we decompose $\hat{X}_0(\omega)$ into two components $X_0(\omega)$ and $\{-i\,\mathrm{sgn}(\omega)\}$, then $\hat{x}_0(t)$, the inverse Fourier transform of $\hat{X}_0(\omega)$, can be given as the convolution of the inverse Fourier transforms of $X_0(\omega)$ and $\{-i\,\mathrm{sgn}(\omega)\}$, respectively. It is straightforward to show that the inverse Fourier transform of $X_0(\omega)$ be $x_0(t)$. However, to obtain the inverse Fourier transform of $\{-i\,\mathrm{sgn}(\omega)\}$ is a little bit cumbersome task.

To this end, we first consider the Fourier trnsform $F_{\mathrm{sgn}}(\omega)$ of the sign function $\mathrm{sgn}(t)$ as follows:

$$\begin{aligned}F_{\mathrm{sgn}}(\omega)&=\int_{-\infty}^{\infty}\mathrm{sgn}(t)\exp -i\omega t\,dt\\&=\int_{-\infty}^{\infty}\mathrm{sgn}(t)\{\cos\omega t-i\sin\omega t\}\,dt\\&=-2i\int_{0}^{\infty}\sin\omega t\,dt\end{aligned}$$

The above integral obviously does not converge in the ordinary sense; however, if it is considered as a distribution,(31) then

$$\begin{aligned}F_{\mathrm{sgn}}(\omega)&=\lim_{T\to\infty}\left[-2i\int_0^T\sin\omega t\,dt\right]\\&=\lim_{T\to\infty}\left[\frac{2(1-\cos\omega T)}{i\omega}\right]=\frac{2}{i\omega}\qquad(\omega\neq0)\end{aligned}$$

At this point, taking inverse Fourier transform of $F_{\mathrm{sgn}}(\omega)$, we can express $\mathrm{sgn}(t)$ in terms of $F_{\mathrm{sgn}}(\omega)$ as

$$\mathrm{sgn}(t)=\frac{1}{2\pi}\int_{-\infty}^{\infty}F_{\mathrm{sgn}}(\omega)\exp i\omega t\,d\omega$$

By replacing t with $-t$ and interchanging t and ω, we get

$$\begin{aligned}2\pi\,\mathrm{sgn}(-\omega)&=-2\pi\,\mathrm{sgn}(\omega)\\&=\int_{-\infty}^{\infty}F_{\mathrm{sgn}}(t)\exp -i\omega t\,dt\\&=\int_{-\infty}^{\infty}\frac{2}{it}\exp -i\omega t\,dt\end{aligned}$$

Hence,

$$-i\,\mathrm{sgn}(\omega)=\int_{-\infty}^{\infty}\frac{1}{\pi t}\exp -i\omega t\,dt$$

This shows that the inverse Fourier transform of $\{-i\,\mathrm{sgn}(\omega)\}$ is equal to $1/(\pi t)$.

Finally, we can see that the Hilbert transform $\hat{x}_0(t)$ of the original record $x_0(t)$ can be given as the convolution of two functions $x_0(t)$ and $1/(\pi t)$, which is exactly of the same form as in Eq. 3. 19.

though $x_0(t)$ is by definition zero in the domains $(-\infty, 0)$ and (T_0, ∞), $\hat{x}_0(t)$ is usually not equal to zero in these domains and therefore the sample functions of the data-based nonstationary random process given by Eq. 3.16 are not necessarily equal to zero outside the domain $[0, T_0]$. It also follows from Eqs. 3.16 and 3.19, that $x(t)$ is not necessarily equal to zero at $t=0$ and T_0 even if $x_0(t)$ is at these time instants. As we shall see later in dealing with earthquake acceleration records, however, $\hat{x}_0(t)$ may be considered approximately zero outside the domain $[0, T_0]$ if the record $x_0(t)$ oscillates rapidly and more or less symmetrically with respect to the base line within the domain $[0, T_0]$.

The following expression alternative to Eq. 3.16 can be written for $x(t)$:

$$x(t) = A_0(t) \cos\{\Phi + \theta_0(t)\} \tag{3.21}$$

where $A_0(t)$ is the envelope function[32]

$$A_0(t) = \sqrt{x_0^2(t) + \hat{x}_0^2(t)} \tag{3.22}$$

and

$$\theta_0(t) = \arctan\{\hat{x}_0(t)/x_0(t)\} \tag{3.23}$$

We now consider the ensemble averages and other characteristics of $x(t)$. In particular, the following quantities are investigated; expected value, autocorrelation function, mean square value and variance, maximum and minimum values, probability density and distribution function and generalized spectra.

Expected Value: With the aid of Eq. 3.16,

$$E\{x(t)\} = x_0(t) \cdot E\{\cos\Phi\} - \hat{x}_0(t) \cdot E\{\sin\Phi\} \tag{3.24}$$

If Φ is uniformly distributed (see Eq. 3.12),

$$E\{x(t)\} = (\sin a/a)\{x_0(t)\cos\mu - \hat{x}_0(t)\sin\mu\} \tag{3.25}$$

which reduces, with $\mu=0$, to

$$E\{x(t)\} = (\sin a/a)x_0(t) \tag{3.26}$$

In addition, if $a=m\pi$ ($m=$ an integer); then

$$E\{\boldsymbol{x}(t)\}=0 \tag{3.27}$$

If Φ has a Gaussian distribution (see Eq. 3.13),

$$E\{\boldsymbol{x}(t)\}=\{x_0(t)\cos\mu-\hat{x}_0(t)\sin\mu\}\exp(-\sigma^2/2) \tag{3.28}$$

which reduces with $\mu=0$ to

$$E\{\boldsymbol{x}(t)\}=x_0(t)\exp(-\sigma^2/2) \tag{3.29}$$

Furthermore, if σ approaches infinity, then

$$E\{\boldsymbol{x}(t)\}=0 \tag{3.30}$$

The following comments are in order at this point: The assumption that Φ is Gaussian with mean μ and standard deviation approaching infinity is equivalent to the assumption that Φ is uniform between $\mu-\pi$ and $\mu+\pi$. This is due to the fact that $\exp i\Phi$ is a periodic function with the period 2π.

We observe from the above that the data-based process can offer a convenience in terms of various forms of the expected value function we can choose.

Antocorrelation Function: The autocorrelation function $R_{xx}(t_1, t_2)$ of $\boldsymbol{x}(t)$ is defined as

$$R_{xx}(t_1, t_2)=E\{\boldsymbol{x}(t_1)\boldsymbol{x}(t_2)\} \tag{3.31}$$

Substituting Eq. 3.16, we obtain

$$\begin{aligned}R_{xx}(t_1,t_2)=&\tfrac{1}{2}\{x_0(t_1)x_0(t_2)+\hat{x}_0(t_1)\hat{x}_0(t_2)\}\\&+\tfrac{1}{2}\{x_0(t_1)x_0(t_2)-\hat{x}_0(t_1)\hat{x}_0(t_2)\}\cdot E\{\cos 2\Phi\}\\&-\tfrac{1}{2}\{x_0(t_1)\hat{x}_0(t_2)+\hat{x}_0(t_1)x_0(t_2)\}\cdot E\{\sin 2\Phi\}\end{aligned} \tag{3.32}$$

If Φ is uniformly distributed,

$$\begin{aligned}R_{xx}(t_1, t_2)=&\tfrac{1}{2}\{x_0(t_1)x_0(t_2)+\hat{x}_0(t_1)\hat{x}_0(t_2)\}\\&+\tfrac{1}{2}\{\sin 2a/(2a)\}\{x_0(t_1)x_0(t_2)-\hat{x}_0(t_1)\hat{x}_0(t_2)\}\cos 2\mu\\&-\tfrac{1}{2}\{\sin 2a/(2a)\}\{x_0(t_1)\hat{x}_0(t_2)+\hat{x}_0(t_1)x_0(t_2)\}\sin 2\mu\end{aligned} \tag{3.33}$$

With $\mu=0$,

$$R_{xx}(t_1,t_2)=\tfrac{1}{2}\{x_0(t_1)x_0(t_2)+\hat{x}_0(t_1)\hat{x}_0(t_2)\}$$
$$+\tfrac{1}{2}\{\sin 2a/(2a)\}\{x_0(t_1)x_0(t_2)-\hat{x}_0(t_1)\hat{x}_0(t_2)\} \quad (3.34)$$

Under the further assumption of $a=m\pi/2$ ($m=$ a positive integer),

$$R_{xx}(t_1,\ t_2)=\tfrac{1}{2}\{x_0(t_1)x_0(t_2)+\hat{x}_0(t_1)\hat{x}_0(t_2)\} \quad (3.35)$$

If Φ is Gaussian,

$$R_{xx}(t_1,t_2)=\tfrac{1}{2}\{x_0(t_1)x_0(t_2)+\hat{x}_0(t_1)\hat{x}_0(t_2)\}$$
$$+\tfrac{1}{2}\exp(-2\sigma^2)[\{x_0(t_1)x_0(t_2)-\hat{x}_0(t_1)\hat{x}_0(t_2)\}\cos 2\mu$$
$$-\{x_0(t_1)\hat{x}_0(t_2)+\hat{x}_0(t_1)x_0(t_2)\}\sin 2\mu] \quad (3.36)$$

With $\mu=0$,

$$R_{xx}(t_1,\ t_2)=\tfrac{1}{2}\{x_0(t_1)x_0(t_2)+\hat{x}_0(t_1)\hat{x}_0(t_2)\}$$
$$+\tfrac{1}{2}\exp(-2\sigma^2)\{x_0(t_1)x_0(t_2)-\hat{x}_0(t_1)\hat{x}_0(t_2)\} \quad (3.37)$$

If, in addition, σ approaches infinity,

$$R_{xx}(t_1,\ t_2)=\tfrac{1}{2}\{x_0(t_1)x_0(t_2)+\hat{x}_0(t_1)\hat{x}_0(t_2)\} \quad (3.38)$$

Mean Square and Variance Functions: The mean square function $R_{xx}(t,\ t)$ of $x(t)$ can be obtained from the autocorrelation function $R_{xx}(t_1,\ t_2)$ by setting $t_1=t_2=t$ while the variance function $\sigma_x^2(t)$ as $R_{xx}(t,\ t)-[E\{x(t)\}]^2$. Hence, using the results derived above, the mean square and variance functions can be written explicitly in terms of $x_0(t)$ and $\hat{x}_0(t)$ under various assumptions with respect to the random variable Φ. Avoiding lengthy writing that would be required for listing all these functions of rather obvious form, we only list at this time the following expression for the variance function

$$\sigma_x^2(t)=\tfrac{1}{2}\{x_0^2(t)+\hat{x}_0^2(t)\} \quad (3.39)$$

This interestingly simple result can be obtained under either the assumption that Φ is uniformly distributed with $\mu=0$ and $a=m\pi$ or the assumption that Φ is Gaussian with $\mu=0$ and $\sigma\to\infty$.

Extreme Values: The maximum and minimum values that $x(t)$ can assume at time t may be evaluated from Eq. 3.21 and these extreme values depend on how the random variable Φ distributes. Indeed, if the distribution of Φ is such that $\cos\{\Phi+\theta_0(t)\}$ can take values of ± 1 (e. g. Φ is uniform between $-\pi$ and π), then

$$\max\{\,|x(t)|\,\}=A_0(t)=\sqrt{x_0^2(t)+\hat{x}_0^2(t)} \qquad (3.40)$$

It is of great practical interest that the extreme value above is equal to the standard deviation $\sigma_x(t)$ multiplied by $\sqrt{2}$ under those conditions through which Eqs. 3.39 and 3.40 are derived:

$$\max\{\,|x(t)|\,\}=\sqrt{2}\,\sigma_x(t) \qquad (3.41)$$

When Φ distributes in any other way, the extreme value must be evaluated accordingly reflecting the characteristics of its distribution. One example of such a case where Φ distributes uniformly between $-\pi/2$ and $\pi/2$ will be considered later.

Probability Density and Distribution Fnnctions: The density function and therefore the distribution function of $x(t)$ at time t depends also on how the random variable Φ distributes. Assuming that Φ distributes uniformly between $-m\pi$ and $m\pi$ ($m=$ a positive integer), we can show that the density function $f_{x(t)}(x)$ of $x(t)$ is symmetric about zero mean and given by

$$\begin{aligned} f_{x(t)}(x) &= 1/\left(\pi\sqrt{A_0^2(t)-x^2}\right) && |x|<A_0(t) \\ &= 0 && |x|>A_0(t) \end{aligned} \qquad (3.42)$$

The corresponding distribution function $F_{x(t)}(x)$ can then be shown to be

$$\begin{aligned} F_{x(t)}(x) &= 0 && x<-A_0(t) \\ &= \tfrac{1}{2}+(1/\pi)\arcsin\,[x/A_0(t)] && |x|\leqq A_0(t) \\ &= 1 && x>A_0(t) \end{aligned} \qquad (3.43)$$

We can also show that the expression in Eq. 3.43 also serves as the distribution function of $x(t)$ when Φ is Gaussian provided that its standard deviation σ approaches infinity and $\mu=0$.

Generalized Spectra: The generalized (power) spectral density $S_{xx}(\omega_1, \omega_2)$ of a nonstationary random process is defined as the (double) Fourier transform(*3) of its autocorrelation function $R_{xx}(t_1, t_2)$:

$$S_{xx}(\omega_1,\omega_2)=(1/2\pi)^2\int_{-\infty}^{\infty}\int_{-\infty}^{\infty}R_{xx}(t_1, t_2)\exp\{-i(\omega_1 t_1-\omega_2 t_2)\}\,dt_1 dt_2 \tag{3.44}$$

By means of inverse transformation,

$$R_{xx}(t_1, t_2)=\int_{-\infty}^{\infty}\int_{-\infty}^{\infty}S_{xx}(\omega_1, \omega_2)\exp\{i(\omega_1 t_1-\omega_2 t_2)\}\,d\omega_1 d\omega_2 \tag{3.45}$$

Using Eq. 3.15 in the definition of the autocorrelation function $R_{xx}(t_1,t_2)=\mathrm{E}\{x(t_1)x(t_2)\}$, we obtain

$$R_{xx}(t_1, t_2)=1/(2\pi)^2\int_{-\infty}^{\infty}\int_{-\infty}^{\infty}X_0(\omega_1)X_0^*(\omega_2)\mathrm{E}\{\exp i\Phi[\mathrm{sgn}(\omega_1)-\mathrm{sgn}(\omega_2)]\}\cdot\exp\{i(\omega_1 t_1-\omega_2 t_2)\}\,d\omega_1 d\omega_2 \tag{3.46}$$

where the superscript * indicates a complex conjugate. Comparison of Eq. 3.46 with Eq. 3.45 leads to

$$S_{xx}(\omega_1, \omega_2)=1/(2\pi)^2 X_0(\omega_1)X_0^*(\omega_2)\mathrm{E}\{\exp i\Phi[\mathrm{sgn}(\omega_1)-\mathrm{sgn}(\omega_2)]\} \tag{3.47}$$

If Φ follows either the uniform bistribution with $a=m\pi$ and $\mu=0$ or the Gaussian distribution $\mu=0$ and $\sigma\to\infty$, the generalized spectrum above reduces to

$$S_{xx}(\omega_1,\omega_2)=\frac{1}{(2\pi)^2}X_0(\omega_1)X_0^*(\omega_2) \qquad 0<\omega_1\omega_2;\ \omega_1=\omega_2=0$$
$$=0 \qquad \text{otherwise} \tag{3.48}$$

Equations 3.47 and 3.48 clearly indicate how the spectral characteristics

(*3) Similar to the Wiener-Khintchine relationship between the autocorrelation function and the corresponding power spectral density for a stationary random process, the constant $1/(2\pi)^2$ is to be placed in the transform from time domain into frequency domain.

of $x_0(t)$ appear in the expressions of the generalized spectrum of $\boldsymbol{x}(t)$. In particular, the simplicity of Eq. 3.48 is of significant practical interest.

Fourier amplitude: The most notable feature of $\boldsymbol{x}(t)$ and its sample functions $x^{(k)}(t)$ is the fact that the Fourier amplitudes of $x^{(k)}(t)$ as well as $\boldsymbol{x}(t)$ are always equal to $|X_0(\omega)|$: The Fourier amplitude of the observation $x_0(t)$ is preserved intact in the proposed data-based nonstationary random process of the first kind and its sample functions.(*4)

In deriving the symmetric density function (Eq. 3.42) for $\boldsymbol{x}(t)$, we have assumed that $\boldsymbol{\Phi}$ has either a uniform density between $-m\pi$ and $m\pi$ or a Gaussian density with mean zero and standard deviation approaching infinity. While the physical phenomena in which we are interested can often be idealized as nonstationary random processes with symmetric distributions as in the case of earthquake acceleration, such symmetry assumptions are obviously not always valid. For example, field measurements of wind-induced pressures on building structures and recorded histories of aircraft acceleration under pilot maneuvers clearly suggest that asymmetric distributions with non-zero mean values are definitely more realistic assumptions. The proposed data-based nonstationary processes can easily simulate such asymmetric observations. If, for example, we assume that $\boldsymbol{\Phi}$ is uniform between $-\pi/2$ and $\pi/2$, it follows from Eqs. 3.26 and 3.33 that

$$E\{\boldsymbol{x}(t)\} = (2/\pi)x_0(t) \tag{3.49}$$

$$R_{\boldsymbol{xx}}(t_1, t_2) = \tfrac{1}{2}\{x_0(t_1)x_0(t_2) + \hat{x}_0(t_1)\hat{x}_0(t_2)\} \tag{3.50}$$

In this case, the distribution function of $\boldsymbol{x}(t)$ becomes asymmetric and is, for $\pi/2 < \theta_0 < 3\pi/2$, given by

$$F_{\boldsymbol{x}(t)}(x) = \{\pi/2 + |\theta_0| - \arccos[x/A_0(t)]\}/\pi \tag{3.51}$$

(*4) It follows from Eq. 3. 11 that

$$|X(\omega)| = |X_0(\omega)\exp i\phi(\omega)| = |X_0(\omega)| \cdot |\exp i\phi(\omega)| = |X_0(\omega)|$$

for $-A_0(t)\cos(\pi/2+|\theta_0|)\geqq x\geqq -A_0(t)\cos(\pi/2-|\theta_0|)$ and

$$F_{X(t)}(x)=1-2\{\arccos[x/A_0(t)]\}/\pi \tag{3.52}$$

for $-A_0(t)\cos(\pi/2-|\theta_0|)\geqq x\geqq -A_0(t)$ where θ_0 is as shown in Eq. 3.23. The assumption of Φ being Gaussian with a finite value of standard deviation also produces an asymmetric distribution of $x(t)$. It appears considerably cumbersome and not particularly of practical value to derive the explicit analytical expression of such an asymmetric distribution function, however.

Unfortunately, if the observation $x_0(t)$ exhibits a highly asymmetric behavior, its Hilbert transform $\hat{x}_0(t)$ is not equal to zero, not even in approximation, in the intervals $(-\infty, 0]$ and $[T_0, \infty)$. Note that these intervals include $t=0$ and $t=T_0$ even when $x_0(t)$ is zero at these two time instants.(*5) Under these conditions, neither can the process $x(t)$ be equal to zero even in approximation in the intervals $(-\infty, 0]$ and $[T_0, \infty)$, while some physical processes of practical importance require that they be equal to zero at the beginning $(t=0)$ and at the end $(t=T_0)$. Indeed, it is this difficulty that motivates the later introduction of *the data-based nonstationary process of the second kind* which always satisfies the requirement.

3.2.2 Multi-variate and one-dimensional processes

The definition of the data-based nonstationary random processes is now extended to the case of multi-variate, but still one-dimensional nonstationary processes. We first consider a set of records $x_{0i}(t)$ $(i=1,2,\cdots\cdots, q)$ all observed in the time interval $[0, T_0]$ describing a temporal observation of a one-dimensional vector quantity $\underline{x}_0(t)$ consisting of q component processes (e.g., EW, NS and vertical components of earthquake accelera-

(*5) Note that the Hilbert transform $\hat{x}_0(t)$ of the original record $x_0(t)$ is given as the convolution of $x_0(t)$ and the function $1/(\pi t)$, as shown in Eq. 3.19.

tion records). On the basis of the records $x_{0i}(t)$, we then construct a q-variate data-based nonstationary process $\underline{\mathbf{x}}(t)$ as

$$\underline{\mathbf{x}}(t)=[x_1(t)\ x_2(t)\cdots\cdots x_q(t)]^{\mathrm{T}} \tag{3.53}$$

with

$$x_i(t)=1/(2\pi)\int_{-\infty}^{\infty}X_{0i}(\omega)\exp i\{\omega t+\phi_i(\omega)\}\,d\omega$$
$$=x_{0i}(t)\cdot\cos\Phi_i-\hat{x}_{0i}(t)\cdot\sin\Phi_i \tag{3.54}$$

$$\phi_i(\omega)=\Phi_i\cdot\mathrm{sgn}\,(\omega) \tag{3.55}$$

where $X_{0i}(\omega)$=Fourier transform of $x_{0i}(t)$, $\hat{x}_{0i}(t)$= Hilbert transform of $x_{0i}(t)$, Φ_i= random variable, not necessarily independent of $\Phi_j(i\neq j)$ and superscript T indicates a transposition.

The expected value (vector) of $\underline{\mathbf{x}}(t)$ is given by

$$\mathrm{E}\{\underline{\mathbf{x}}(t)\}=[\mathrm{E}\{x_1(t)\}\ \mathrm{E}\{x_2(t)\}\cdots\cdots\mathrm{E}\{x_q(t)\}]^{\mathrm{T}} \tag{3.56}$$

for which the expressions similar to Eqs. 3.25 —3.30 follow depending on he type of distribution function assumed for the random variables Φ_i's.

One of the most important characteristics of multi-variate random protcesses is the correlation among the component processes, which in the present case finds its origin in the statistical dependence among Φ_i's. Primarily for brevity, we assume here that the marginal distribution functions of Φ_i's are either all identical with a uniform density between $-m\pi$ and $m\pi$ or all Gaussian with zero mean and possibly different values of standard deviation.

For those Φ_i's distributed uniformly, two extreme modes of their statistical dependence are considered. One of these represents the state of complete independence where all Φ_i's are independent of each other while the other represents a special form of total dependence in which all Φ_i's are identical ($\Phi_1=\Phi_2=\cdots\cdots=\Phi_q=\Phi$). Intermediate modes of dependence are not considered since the joint density functions which involve Φ_i's and produce uniform marginal distributions for Φ_i's appear to be extremely difficult to obtain. However, when all Φ_i's are Gaussian, arbitrary degrees of dependence (including those cases of complete independence and total dependence described above) can easily be introduced through the wellknown Gaussian joint density functions involving Φ_i's. This fact is one definite advantage the Gaussian assumption can enjoy over the assumption of uniform distribution.

The crosscorrelation function matrix $\underline{R}_{\mathbf{xx}}(t_1, t_2)$ of $\underline{\mathbf{x}}(t)$ is by definition

$$\underline{R}_{\mathbf{xx}}(t_1,t_2)=\begin{pmatrix} R_{\boldsymbol{x}_1\boldsymbol{x}_1}(t_1, t_2) & R_{\boldsymbol{x}_1\boldsymbol{x}_2}(t_1, t_2) & \cdots\cdots & R_{\boldsymbol{x}_1\boldsymbol{x}_q}(t_1, t_2) \\ R_{\boldsymbol{x}_2\boldsymbol{x}_1}(t_1, t_2) & \cdots\cdots & \cdots\cdots & \cdots\cdots \\ \cdots\cdots & \cdots\cdots & \cdots\cdots & \cdots\cdots \\ \cdots\cdots & \cdots\cdots & \cdots\cdots & \cdots\cdots \\ \cdots\cdots & \cdots\cdots & \cdots\cdots & \cdots\cdots \\ R_{\boldsymbol{x}_q\boldsymbol{x}_1}(t_1, t_2) & \cdots\cdots & \cdots\cdots & R_{\boldsymbol{x}_q\boldsymbol{x}_q}(t_1, t_2) \end{pmatrix} \tag{3.57}$$

where the crosscorrelation functions $R_{\boldsymbol{x}_i\boldsymbol{x}_j}(t_1, t_2)$ are in turn defined as

$$R_{\boldsymbol{x}_i\boldsymbol{x}_j}(t_1, t_2)=\mathrm{E}\{\boldsymbol{x}_i(t_1)\boldsymbol{x}_j(t_2)\} \tag{3.58}$$

Obviously, Eq. 3.58 gives the autocorrelation function when $i=j$. As two alternative forms (Eqs. 3.32 and 3.46) exist for the autocorrelation function $R_{\boldsymbol{xx}}(t_1, t_2)$ in the uni-variate case, we have the following two equivalent expressions for $R_{\boldsymbol{x}_i\boldsymbol{x}_j}(t_1, t_2)$:

$$\begin{aligned} R_{\boldsymbol{x}_i\boldsymbol{x}_j}(t_1, t_2)=&\,x_{0i}(t_1)x_{0j}(t_2)\cdot\mathrm{E}\{\cos\Phi_i\cdot\cos\Phi_j\} \\ &+\hat{x}_{0i}(t_1)\hat{x}_{0j}(t_2)\cdot\mathrm{E}\{\sin\Phi_i\cdot\sin\Phi_j\} \\ &-\hat{x}_{0i}(t_1)x_{0j}(t_2)\cdot\mathrm{E}\{\sin\Phi_i\cdot\cos\Phi_j\} \\ &-x_{0i}(t_1)\hat{x}_{0j}(t_2)\cdot\mathrm{E}\{\cos\Phi_i\cdot\sin\Phi_j\} \end{aligned} \tag{3.59}$$

and

$$R_{x_i x_j}(t_1, t_2) = 1/(2\pi)^2 \int_{-\infty}^{\infty} \int_{-\infty}^{\infty} X_{0i}(\omega_1) X_{0j}^*(\omega_2)$$
$$\times E\{\exp\ i[\Phi_i \operatorname{sgn}(\omega_1) - \Phi_j \operatorname{sgn}(\omega_2)]\} \cdot \exp\{i(\omega_1 t_1 - \omega_2 t_2)\} d\omega_1 d\omega_2 \tag{3.60}$$

Equations 3.59 and 3.60 take various forms similar to Eqs. 3.33—3.38 depending on whether the distribution functions of Φ_i's are uniform or Gaussian.

If we assume that all Φ_i's are uniformly distributed between $-m\pi$ and $m\pi$ and independent of each other, then the expected value $E\{x_i(t)\} = 0$ and the crosscorrelation function $R_{x_i x_j}(t_1, t_2) = 0$ $(i \neq j)$ while the autocorrelation function $R_{x_i x_i}(t_1, t_2)$ takes the form of Eq. 3.35 with $x_{0i}(t)$ replacing $x_0(t)$. In this case, therefore, the crosscorrelation matrix $\mathrm{R}_{\mathbf{xx}}(t_1, t_2)$ becomes diagonal. On the other hand, if Φ_i 's are all fully correlated $(\Phi_1 = \Phi_2 = \cdots\cdots = \Phi_q = \Phi)$, the expected value $E\{x_i(t)\} = 0$ while the autocorrelation function $(i = j)$ and crosscorrelation function $(i \neq j)$ are both given by

$$R_{x_i x_j}(t_1, t_2) = \tfrac{1}{2}\{x_{0i}(t_1) x_{0j}(t_2) + \hat{x}_{0i}(t_1) \hat{x}_{0j}(t_2)\} \tag{3.61}$$

If we assume that all Φ_i' s are Gaussian with zero mean, the joint density function can be written as

$$f_{\Phi_i \Phi_j}(x, y) = 1/(2\pi \sqrt{1 - \rho_{ij}^2}\,\sigma_i \sigma_j)$$
$$\times \exp[-\tfrac{1}{2}\{(x/\sigma_i)^2 - 2\rho_{ij} xy/(\sigma_i \sigma_j) + (y/\sigma_j)^2\}/(1 - \rho_{ij}^2)] \tag{3.62}$$

where σ_i = standard deviation of Φ_i and ρ_{ij} = coefficient of correlation between Φ_i and Φ_j. Then, the expected value $E\{x_i(t)\}$ is given by Eq. 3.29 and the autocorrelation function $R_{x_i x_i}(t_1, t_2)$ by Eq. 3.37 with $x_{0i}(t)$ and σ_i respectively replacing $x_0(t)$ and σ, while the crosscorrelation function $R_{x_i x_j}(t_1, t_2)$ $(i \neq j)$ takes the form:

$$R_{x_i x_j}(t_1, t_2) = \tfrac{1}{2}\{x_{0i}(t_1) x_{0j}(t_2) + \hat{x}_{0i}(t_1) \hat{x}_{0j}(t_2)\}$$

$$\times \exp\{-(\sigma_i^2 - 2\rho_{ij}\sigma_i\sigma_j + \sigma_j^2)/2\}$$
$$+\tfrac{1}{2}\{x_{0i}(t_1)x_{0j}(t_2) - \hat{x}_{0i}(t_1)\hat{x}_{0j}(t_2)\}$$
$$\times \exp\{-(\sigma_i^2 + 2\rho_{ij}\sigma_i\sigma_j + \sigma_j^2)/2\} \quad (3.63)$$

If we impose the assumption that $\rho_{ij}=0\ (i\neq j)$ or equivalently that Φ_i's are independent of each other, the expected value $E\{x_i(t)\}$ and the autocorrelation function $R_{x_ix_i}(t_1, t_2)$ remain respectively of the form of Eqs. 3.29 and 3.37, while the crosscorrelation function $R_{x_ix_j}(t_1, t_2)(i\neq j)$ becomes

$$R_{x_ix_j}(t_1,t_2)=x_{0i}(t_1)x_{0j}(t_2)\exp\{-(\sigma_i^2+\sigma_j^2)/2\} \quad (3.64)$$

Furthemore, if we let σ_i $(i=1, 2, \cdots\cdots, q)$ approach infinity, it follows that the expected value $E\{x_i(t)\}=0$, the crosscorrelation function $R_{x_ix_j}(t_1, t_2)=0\ (i\neq j)$ and the autocorrelation function $R_{x_ix_i}(t_1, t_2)$ is given by Eq. 3.38 with $x_{0i}(t)$ replacing $x_0(t)$. Therefore, as in the case of uniform Φ_i's, the crosscorrelation function matrix becomes diagonal when Φ_i's are Gaussian with $\rho_{ij}=0\ (i\neq j)$ and $\sigma_i\to\infty$ $(i=1, 2, \cdots\cdots, q)$.

If all Φ_i's are Gaussian but fully correlated $(\Phi_1=\Phi_2=\cdots\cdots=\Phi_q=\Phi)$ and hence $\sigma_1=\sigma_2=\cdots\cdots=\sigma_q=\sigma$, the following crosscorrelation functions are obtained from Eq. 3.63 with ρ_{ij} being replaced by unity:

$$R_{x_ix_j}(t_1, t_2)=\tfrac{1}{2}\{x_{0i}(t_1)x_{0j}(t_2)+\hat{x}_{0i}(t_1)\hat{x}_{0j}(t_2)\}$$
$$+\tfrac{1}{2}\exp(-2\sigma^2)\{x_{0i}(t_1)x_{0j}(t_2)-\hat{x}_{0i}(t_1)\hat{x}_{0j}(t_2)\} \quad (3.65)$$

In this case, the expected value and the autocorrelation function take the same forms as those for the completely independent case: Eq. 3.29 for the expected value and Eq. 3.37 for the autocorrelation function with $x_{0i}(t)$ replacing $x_0(t)$. If, moreover, σ approaches infinity $(i=1, 2, \cdots\cdots, q)$, the expected value $E\{x_i(t)\}=0$ and the autocorrelation function $R_{x_ix_i}(t_1, t_2)$ is given by Eq. 3.38 with $x_{0i}(t)$ replacing $x_0(t)$ while the crosscorrelation function becomes

$$R_{x_ix_j}(t_1,\ t_2)=\tfrac{1}{2}\{x_{0i}(t_1)x_{0j}(t_2)+\hat{x}_{0i}(t_1)\hat{x}_{0j}(t_2)\} \tag{3.66}$$

Note that the last equation is identical to Eq. 3.61.

Extending now the definition of the generalized spectrum $S_{xx}(\omega_1,\ \omega_2)$ into the case of multi-variate processes, we define the generalized cross-spectral density matrix $\underline{S}_{\mathbf{XX}}(\omega_1,\omega_2)$ as

$$\underline{S}_{\mathbf{XX}}(\omega_1,\omega_2)=\begin{bmatrix} S_{x_1x_1}(\omega_1,\ \omega_2) & S_{x_1x_2}(\omega_1,\ \omega_2) & \cdots & S_{x_1x_q}(\omega_1,\ \omega_2) \\ S_{x_2x_1}(\omega_1,\ \omega_2) & \cdots & \cdots & \cdots \\ \cdots & \cdots & \cdots & \cdots \\ S_{x_qx_1}(\omega_1,\ \omega_2) & \cdots & \cdots & S_{x_qx_q}(\omega_1,\ \omega_2) \end{bmatrix} \tag{3.67}$$

where the (generalized) cross-spectral density function $S_{x_ix_j}(\omega_1,\ \omega_2)$ is given as the double Fourier transform of $R_{x_ix_j}(t_1,\ t_2)$:

$$S_{x_ix_j}(\omega_1,\ \omega_2)=1/(2\pi)^2\int_{-\infty}^{\infty}\int_{-\infty}^{\infty}R_{x_ix_j}(\omega_1,\ \omega_2)\exp\{-i(\omega_1t_1-\omega_2t_2)\}dt_1dt_2 \tag{3.68}$$

which produces the generalized spectral density $S_{x_ix_i}(\omega_1,\omega_2)$ of $x_i(t)$ when $i=j$. By means of the inverse Fourier transform, we obtain

$$R_{x_ix_j}(t_1,\ t_2)=\int_{-\infty}^{\infty}\int_{-\infty}^{\infty}S_{x_ix_j}(\omega_1,\ \omega_2)\exp\{i(\omega_1t_1-\omega_2t_2)\}\,d\omega_1d\omega_2 \tag{3.69}$$

Comparing Eq. 3.69 with Eq. 3.60, we conclude that

$$S_{x_ix_j}(\omega_1,\omega_2)=(1/2\pi)^2X_{0i}(\omega_1)X_{0j}^{*}(\omega_2)\cdot E[\exp i\{\Phi_i\,\mathrm{sgn}(\omega_1)-\Phi_j\,\mathrm{sgn}(\omega_2)\}] \tag{3.70}$$

Again depending on whether Φ_i is uniformly distributed or Gaussian, various forms of the cross-spectral density function will emerge from Eq. 3.70. As mentioned earlier, the appropriate joint density functions with uniform marginal densities appear to be unavailable at this time. Therefore, we concentrate in the present study on the case where Φ_i's are jointly distributed as Gaussian. As before, we further assume that the mean value and the standard deviation of Φ_i are respectively zero and σ_i ($i=1, 2, \cdots\cdots, q$). This assumption makes the cross-spectral density function relatively simple as shown below without sacrificing its usefulness in applications.

$$S_{\boldsymbol{x}_i\boldsymbol{x}_j}(\omega_1, \omega_2)=(1/2\pi)^2 X_{0i}(\omega_1)X^*_{0j}(\omega_2)\cdot\exp\{-\tfrac{1}{2}(\sigma_i^2+2\delta\rho_{ij}\sigma_i\sigma_j+\sigma_j^2)\} \tag{3.71}$$

where $\delta=-1$ if $\omega_1\omega_2>0$ and $\delta=1$ if $\omega_1\omega_2<0$. Eq. 3.71 is valid also for $i=j$ if we set $\rho_{ij}=1$.

In the special case of the complete independence ($\rho_{ij}=0$ for $i\neq j$), we have

$$S_{\boldsymbol{x}_i\boldsymbol{x}_j}(\omega_1, \omega_2)=(1/2\pi)^2 X_{0i}(\omega_1)X^*_{0j}(\omega_2)\cdot\exp\{-\tfrac{1}{2}(\sigma_i^2+\sigma_j^2)\} \tag{3.72}$$

and for $i=j$, we have $\rho_{ij}=1$ and hence

$$S_{\boldsymbol{x}_i\boldsymbol{x}_i}(\omega_1, \omega_2)=(1/2\pi)^2 X_{0i}(\omega_1)X^*_{0i}(\omega_2)\exp\{-\tfrac{1}{2}(1+\delta)^2\sigma_i^2\} \tag{3.73}$$

Therefore, the following diagonal cross-spectral density matrix follows from the further assumption of $\sigma_i\to\infty$ ($i=1, 2, \cdots\cdots, q$);

$$\underline{S}_{\mathbf{XX}}(\omega_1, \omega_2)=\frac{(1-\delta)}{2(2\pi)^2}\begin{pmatrix} X_{01}(\omega_1)X^*_{01}(\omega_2) & & \cdots\cdots & 0 \\ 0 & X_{02}(\omega_1)X^*_{02}(\omega_2) & \cdots\cdots & 0 \\ \cdot & & & \cdot \\ \cdot & & & \cdot \\ 0 & \cdots\cdots & \cdots\cdots & X_{0q}(\omega_1)X^*_{0q}(\omega_2) \end{pmatrix} \tag{3.74}$$

We note again that Eq. 3.74 is valid under $\rho_{ij}=0$, $\sigma_i\to\infty$, $\delta=-1$ for $\omega_1\omega_2>0$, and $\delta=1$ for $\omega_1\omega_2<0$.

In the case of full correlation where $\Phi_1=\Phi_2=\cdots\cdots=\Phi_q=\Phi$ and hence $\sigma_1=\sigma_2=\cdots\cdots=\sigma_q=\sigma$, the cross-spectral densities are

$$S_{x_i x_j}(\omega_1,\omega_2)=(1/2\pi)^2 X_{0i}(\omega_1)X_{0j}^*(\omega_2)\cdot\exp\{-\tfrac{1}{2}(1+\delta)^2\sigma^2\} \tag{3.75}$$

which is valid whether $i=j$ or $i\neq j$. If, furthermore, $\sigma\to\infty$, we obtain

$$\mathbf{S}_{\mathbf{xx}}(\omega_1,\omega_2)=\frac{(1-\delta)}{2(2\pi)^2}\begin{bmatrix} X_{01}(\omega_1)X_{01}^*(\omega_2) & X_{01}(\omega_1)X_{02}^*(\omega_2)\cdots\cdots & X_{01}(\omega_1)X_{0q}^*(\omega_2) \\ X_{02}(\omega_1)X_{01}^*(\omega_2) & \cdots\cdots & \cdots\cdots \\ \cdots\cdots & \cdots\cdots & \cdots\cdots \\ \cdots\cdots & \cdots\cdots & \cdots\cdots \\ X_{0q}(\omega_1)X_{01}^*(\omega_2) & \cdots\cdots & X_{0q}(\omega_1)X_{0q}^*(\omega_2) \end{bmatrix} \tag{3.76}$$

The mean square and variance functions, extreme values, probability density and distribution functions of the component process $x_i(t)$ can be evaluated in the same way as those of the univariate process $x(t)$.

3. 3 Data-Based Nonstationary Random Processes of the Second Kind

3. 3. 1 Introduction

Some physical processes of engineering importance initiate and terminate with zero values as exemplified by earthquake acceleration records. Unfortunately, as pointed out earlier, when the record $x_0(t)$ observed in the interval $[0, T_0]$ does not oscillate rapidly and at the same time more or less symmetrically with respect to the base line, again as exemplified by earthquake acceleration records, the data-based nonstationary random processes of the first kind and their sample functions fail to satisfy the zero initial and terminal conditions even in approximation. We can show however that a relatively simple modification alters the characteristics of these processes of the first kind leading us to a family of nonstationary random processes whose sample functions always satisfy the initial and terminal conditions rigorously. This family is referred to as *the data-based nonstationary random processes of the second kind*. It is pointed out however that the modification is not achieved without penalty. Indeed, the processes of the second kind and their sample functions can observe the preservation of the Fourier amplitude $|X_0(\omega)|$ of the original record $x_0(t)$ only in approximation. Nonetheless, in view of the fact that in practice we often deal with the processes which either by nature or by definition must have zero initial and terminal values, the data-based nonstationary random processes of the second kind are introduced and their characteristics examined in the following, restricting, however, our attention only to the uni-variate cases in the present study.

3. 3. 2 Preliminary Analysis

A record $x_0(t)$ of duration T_0 is again considered. By definition, the record begins at $t=0$ and terminates at $t=T_0$ with its value being identically equal to zero outside the interval $[0, T_0]$. We then construct the symmetric extension $y_0(t)$ of $x_0(t)$:

$$y_0(t)=x_0(t)+x_0(-t) \tag{3.77}$$

We further construct the periodic extension of $z_N(t)$ of $y_0(t)$:

$$z_N(t)=\sum_{k=-N}^{N} y_0(t-2kT_0) \tag{3.78}$$

Three functions $x_0(t)$, $y_0(t)$ and $z_N(t)$ are schematically illustrated in Figs. 1, 2 and 3 respectively. Note that $y_0(t)$ and $z_N(t)$ are symmetric with respect to the origin. The Fourier transforms $Y_0(\omega)$ of $y_0(t)$ and $Z_N(\omega)$ of $z_N(t)$ can be shown as

$$Y_0(\omega)=Y_0(-\omega)=X_0(\omega)+X_0^*(\omega)=2\,\mathrm{Re}\,[X_0(\omega)] \tag{3.79}$$

$$Z_N(\omega)=Z_N(-\omega)=Y_0(\omega)p_N(\omega) \tag{3.80}$$

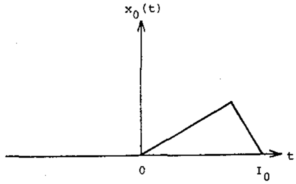

Fig. 1 A record $x_0(t)$

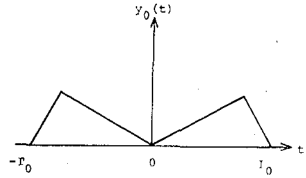

Fig. 2 Symmetric extension $y_0(t)$ of $x_0(t)$

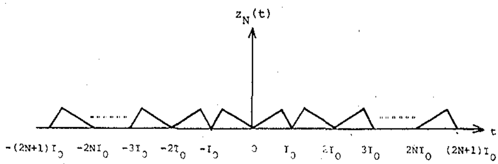

Fig. 3 Periodic extension $z_N(t)$ of $y_0(t)$

where $p_N(\omega)$ is a periodic function (with period $\omega_0=\pi/T_0$) known as the Fourier-series kernel:

$$p_N(\omega)=\sum_{k=-N}^{N}\exp(i\,2\,kT_0\omega)=\{\sin(2N+1)T_0\omega\}/\sin(T_0\omega)$$

$$=p_N(-\omega) \qquad (3.81)$$

We can show that as $N\to\infty$ and for $(k-½)\omega_0\leqq\omega\leqq(k+½)\omega_0$

$$\lim_{N\to\infty}p_N(\omega)=\omega_0\delta(\omega-k\omega_0) \qquad (3.82)$$

Therefore, we obtain, as (※6) $N\to\infty$, from Eqs. 3.81

(*6) Since $p_N(\omega)$ is periodic with period $\omega_0=\pi/T_0$, if we show that, in the interval $(-\omega_0/2,\ \omega_0/2)$, $p_N(\omega)$ tends to $\omega_0\delta(\omega)$, it will follow that

$$\lim_{N\to\infty}p_N(\omega)=\omega_0\sum_{k=-\infty}^{\infty}\delta(\omega-k\omega_0)$$

From Eq. 3. 81 we have

$$p_N(\omega)=\frac{\sin(2N+1)T_0\omega}{\sin(T_0\omega)}=\frac{\sin(2N+1)T_0\omega}{\pi\omega}\cdot\frac{T_0\omega}{\sin(T_0\omega)}\cdot\omega_0$$

But we see(31) that

$$\lim_{N\to\infty}\frac{\sin(2N+1)T_0\omega}{\pi\omega}=\delta(\omega)$$

and since $T_0\omega/\sin(T_0\omega)$ is bounded in the $(-\omega_0/2,\ \omega_0/2)$ interval we conclude that for $|\omega|<\omega_0/2$

$$\lim_{N\to\infty} p_N(\omega)=\omega_0\sum_{k=-\infty}^{\infty}\delta(\omega-k\omega_0) \tag{3.83}$$

and from Eq. 3.80,

$$Z_0(\omega)=\lim_{N\to\infty} Z_N(\omega)=\omega_0\sum_{k=-\infty}^{\infty} Y_0(k\omega_0)\delta(\omega-k\omega_0) \tag{3.84}$$

Defining $z_0(t)$ as

$$z_0(t)=\lim_{N\to\infty}\sum_{k=-N}^{N} y_0(t-2kT_0) \tag{3.85}$$

we observe that $z_0(t)$ and $Z_0(\omega)$ constitute a Fourier transform pair. It is noted that $Z_0(\omega)$ is a real and even function of ω.

Introducing a temporal filter of the form

$$\begin{aligned} v(t)=U(t)-U(t-T_0)&=1 \qquad 0<t<T_0 \\ &=0 \qquad t<0;\ t>T_0 \end{aligned} \tag{3.86}$$

with $U(t)$ inicating the Heavyside unit step function, we may write

$$x_0(t)=z_0(t)\cdot v(t) \tag{3.87}$$

The Fourier transform $X_0(\omega)$ of $x_0(t)$ can then be written as (*7)

$$\begin{aligned} X_0(\omega)&=1/(2\pi)\int_{-\infty}^{\infty} Z_0(\lambda)V(\omega-\lambda)\,d\lambda \\ &=P_0(\omega)+Q_0(\omega) \end{aligned} \tag{3.88}$$

where $V(\omega)$ is the Fourier transform of the temporal filter $v(t)$,

$$\begin{aligned} V(\omega)&=\int_{-\infty}^{\infty} v(t)\exp(-i\omega t)dt=(2/\omega)\sin(T_0\omega/2)\cdot\exp(-iT_0\omega/2) \\ &=(1/\omega)[\sin\omega T_0-2i\sin^2(\omega T_0/2)] \end{aligned} \tag{3.89}$$

$$\begin{aligned} \lim_{N\to\infty} p_N(\omega)&=\omega_0\cdot\frac{T_0\omega}{\sin(T_0\omega)}\cdot\delta(\omega) \\ &=\omega_0\cdot\frac{T\omega_0}{\sin(T_0\omega)}\Big|_{\omega=0}\cdot\delta(\omega) \\ &=\omega_0\delta(\omega) \end{aligned}$$

(*7) It follows from the frequency convolution theorem that the Fourier transform $F(\omega)$ of the product $f_1(t)f_2(t)$ of two functions equals the convolution $F_1(\omega)*F_2(\omega)$ of their respective transforms $F_1(\omega)$ and $F_2(\omega)$ divided by 2π.

$$P_0(\omega) = 1/(2\pi)\int_0^{\infty} Z_0(\lambda)V(\omega+\lambda)\,d\lambda \tag{3.90}$$

$$Q_0(\omega) = 1/(2\pi)\int_0^{\infty} Z_0(\lambda)V(\omega-\lambda)\,d\lambda \tag{3.91}$$

The Fourier transform pairs listed below are useful in the analysis that follows (see also footnote (*2)):

(a) $w_e(t) = U(t+T_0) - U(t-T_0)$ (see Fig. 4)

$W_e(\omega) = W_e(-\omega) = (2/\omega)\sin\omega T_0$ (real) (3.92)

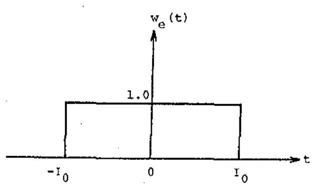

Fig. 4 An even temporal filter $w_e(t)$

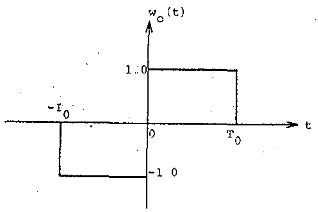

Fig. 5 An odd temporal filter $w_o(t)$

(b) $w_o(t) = w_e(t)\cdot\mathrm{sgn}(t)$ (see Fig. 5)

$W_o(\omega) = -W_o(-\omega) = -(4i/\omega)\sin^2(\omega T_0/2)$ (imaginary) (3.93)

(c) $U(t) = ½ + ½\,\mathrm{sgn}(t)$ (unit step function)

$\overline{U}(\omega) = \pi\delta(\omega) + 1/(i\omega)$ (3.94)

(d) $\overline{U}_1(t) = ½[\delta(t) - 1/(i\pi t)]$

$U(\omega) = ½ + ½\,\mathrm{sgn}(\omega)$ (unit step function,real) (3.95)

(e) $\overline{U}_2(t) = ½[\delta(t) + 1/(i\pi t)]$

$U(-\omega) = ½ - ½\,\mathrm{sgn}(\omega)$ (real) (3.96)

Substituting the last member of Eq. 3.89 into Eq. 3.91 and using $W_e(\omega)$ and $W_o(\omega)$ defined in Eqs. 3.92 and 3.93, we obtain

$$\begin{aligned} Q_0(\omega) &= 1/(4\pi)\int_{-\infty}^{\infty} Z_0(\lambda)U(\lambda)W_e(\omega-\lambda)\,d\lambda \\ &\quad + 1/(4\pi)\int_{-\infty}^{\infty} Z_0(\lambda)U(\lambda)W_o(\omega-\lambda)\,d\lambda \\ &= 1/(2\pi)\int_{-\infty}^{\infty} Z_0(\lambda)U(\lambda)V(\omega-\lambda)\,d\lambda \end{aligned} \tag{3.97}$$

or equivalently

$$Q_0(\omega)=\tfrac{1}{2}[1/(2\pi)\{Z_0(\omega)U(\omega)\}*W_e(\omega)] \\ +\tfrac{1}{2}[1/(2\pi)\{Z_0(\omega)U(\omega)\}*W_o(\omega) \\ =1/(2\pi)\{Z_0(\omega)U(\omega)\}*V(\omega) \tag{3.98}$$

where the asterisk indicates a convolution integral. The inverse Fourier transform of $Z_0(\omega)U(\omega)$ is given by the convolution of $z_0(t)$ and $\overline{U}_1(t)=\tfrac{1}{2}\{\delta(t)-1/(i\pi t)\}$ (see Eq. 3.95):

$$q_{01}(t)=z_0(t)*[\tfrac{1}{2}\{\delta(t)-1/(i\pi t)\}] \\ =\tfrac{1}{2}\{z_0(t)+i\hat{z}_0(t)\} \tag{3.99}$$

where the fact has been used that the Hilbert transform $\hat{z}_0(t)$ of $z_0(t)$ is given by

$$\hat{z}_0(t)=z_0(t)*[1/(\pi t)] \tag{3.100}$$

Similarly, with the aid of Eq. 3.96, we obtain the inverse Fourier transform of $Z_0(\omega)U(-\omega)$ as

$$q_{02}(t)=z_0(t)*[\tfrac{1}{2}\{\delta(t)+1/(i\pi t)\}]=\tfrac{1}{2}\{z_0(t)-i\hat{z}_0(t)\} \tag{3.101}$$

Recognizing that Eq. 3.97 also consists of two convolution integrals involving $q_{01}(t)$, q_{02}(t), $w_e(t)$ and $w_o(t)$, we conclude that the Fourier inverse transform $q_0(t)$ of $Q_0(\omega)$ is

$$q_0(t)=\tfrac{1}{2}\{z_0(t)+i\hat{z}_0(t)\}v(t) \tag{3.102}$$

Similarly, the Fourier inverse transform $p_0(t)$ of $P_0(\omega)$ is

$$p_0(t)=\tfrac{1}{2}\{z_0(t)-i\hat{z}_0(t)\}v(t) \tag{3.103}$$

Writing $P_0(\omega)$ in a form similar to Eq. 3.98, and comparing, we can show that

$$P_0(-\omega)=Q_0^*(\omega),\ Q_0(-\omega)=P_0^*(\omega) \tag{3.104}$$

3. 3. 3 Construction of the Processes of the Second Kind

Now construct a nonstationary random process $z(t)$ on the basis of $z_0(t)$ which is the symmetric-periodic extension of the original record $x_0(t)$ as introduced in the preceding section:

$$z(t)=1/(2\pi)\int_{-\infty}^{\infty}Z_0(\omega)\exp i\{\omega t+\Phi\cdot\mathrm{sgn}(\omega)\}\,d\omega \qquad (3.105)$$

The similarity between the process $x(t)$ of the first kind defined by Eqs. 3.7—a and 3.9 and the process $z(t)$ above is selfevident. Similar to Eq. 3.16, the following expression can then be derived for $z(t)$ from Eq. 3.105:

$$z(t)=z_0(t)\cos\Phi-\hat{z}_0(t)\sin\Phi \qquad (3.106)$$

where $\hat{z}_0(t)$ is the Hilbert transform of $z_0(t)$. The Fourier transform of $\hat{Z}_0(\omega)$ of $\hat{z}_0(t)$ is obtained (see Eq. 3.20) as

$$\hat{Z}_0(\omega)=-i\,\mathrm{sgn}(\omega)\cdot Z_0(\omega) \qquad (3.107)$$

and therefore

$$\hat{z}_0(t)=1/(2\pi)\int_{-\infty}^{\infty}\hat{Z}_0(\omega)\exp(i\omega t)\,d\omega \qquad (3.108)$$

or equivalently (see Eq. 3.18),

$$\hat{z}_0(t)=1/\pi\int_{0}^{\infty}Z_0(\omega)\sin\omega t\,d\omega \qquad (3.109)$$

We can also show that the process $z(t)$ and its sample functions preserve the Fourier amplitude $|Z_0(\omega)|$ of the extended record $z_0(t)$ just as the process $x(t)$ of the first kind and its sample functions have preserved $|X_0(\omega)|$.

The data-based nonstationary random process $x(t)$ of the second kind is now defined as

$$x(t)=z(t)\cdot v(t)=x_0(t)\cos\Phi-\tilde{x}_0(t)\sin\Phi \qquad (3.110)$$

where $x_0(t)=z_0(t)\cdot v(t)$ is the original record and

$$\tilde{x}_0(t)=\hat{z}_0(t)\cdot v(t) \qquad (3.111)$$

Thus, the process $x(t)$ of the second kind is nothing but that segment of $z(t)$ which extends over the interval $[0, T_0]$. The Fourier transform $\tilde{X}_0(\omega)$ of $\tilde{x}_0(t)$ is obtained (see Eq. 3.107) as

$$\tilde{X}_0(\omega)=1/(2\pi)\hat{Z}_0(\omega)*V(\omega)=-i/(2\pi)[\mathrm{sgn}(\omega)\cdot Z_0(\omega)]*V(\omega) \qquad (3.112)$$

which after some algebraic manipulation becomes

$$\tilde{X}_0(\omega)=i\{P_0(\omega)-Q_0(\omega)\} \tag{3.113}$$

With respect to $x(t)$ of the second kind, the following observation is of crucial importance: From the time domain definition of the Hilbert transformation (Eq. 3.19), it follows that the Hilbert transform $\hat{z}_0(t)$ of $z_0(t)$ and therefore $\tilde{x}_0(t)$ are equal to zero at $t=0$ and $t=T_0$ since $z_0(t)$ is a symmetric function of time with respect to these time instants (see Fig. 3). In addition, if the original process $x_0(t)$ is equal to zero at $t=0$ and $t=T_0$, then, by virtue of Eq. 3.110, $x(t)$ is also equal to zero at the same time instants. Comparing Eq. 3.110 with Eq. 3.16 and realizing that in both cases the randomness is introduced through Φ, we conclude that the expressions for the expected value, autocorrelation function, mean square and variance functions, extreme values, probability density and distribution functions derived for the process of the first kind are also valid for the process of the second kind if we replace $\hat{x}_0(t)$ by $\tilde{x}_0(t)$ in those expressions. However, the expressions for the generalized spectra and the Fourier amplitude must be modified.

The Fourier transform $X(\omega)$ of the processes of the second kind is obtained from the second member of Eq. 3.110 as

$$X(\omega)=1/(2\pi)[Z(\omega)*V(\omega)] \tag{3.114}$$

This equation, with the aid of Eq. 3.105, can be rewritten as

$$\begin{aligned} X(\omega) &= 1/(2\pi)[Z_0(\omega)\exp\{i\Phi\,\mathrm{sgn}\,(\omega)\}]*V(\omega) \\ &= [1/(2\pi)\{Z_0(\omega)U(\omega)\}*V(\omega)]\exp(i\Phi) \\ &\quad +[1/(2\pi)\{Z_0(\omega)U(-\omega)\}*V(\omega)]\exp(-i\Phi) \end{aligned} \tag{3.115}$$

which, with the further aid of Eq. 3.98 for $Q_0(\omega)$ and corresponding expression for $P_0(\omega)$, finally becomes

$$X(\omega)=P_0(\omega)\exp(-i\Phi)+Q_0(\omega)\exp(i\Phi) \tag{3.116}$$

The result shown in Eq. 3.116 can also be arrived at by taking the Fourier transform of the third member of Eq. 3.110

$$X(\omega)=X_0(\omega)\cos\Phi-\tilde{X}_0(\omega)\sin\Phi \tag{3.117}$$

and using Eqs. 3.88 and 3.113 for $X_0(\omega)$ and $\tilde{X}_0(\omega)$. Comparison of Eq. 3.116 with Eq. 3.88 unfortunately indicates that for the process of the second kind, no identity exists either between the Fourier transforms, $X_0(\omega)$ and $X(\omega)$, nor between the Fourier amplitudes, $|X_0(\omega)|$ and $|X(\omega)|$:

$$X_0(\omega)\neq X(\omega), \qquad |X_0(\omega)|\neq|X(\omega)| \tag{3.118}$$

More specifically, using Eqs. 3.88, 3.104 and 3.116, we obtain

$$|X_0(\omega)|^2=|P_0(\omega)|^2+|Q_0(\omega)|^2+2\,\mathrm{Re}[P_0(\omega)P_0(-\omega)] \tag{3.119}$$

and

$$|X(\omega)|^2=|X_0(\omega)|^2-P_0(\omega)P_0(-\omega)\{1-\exp(-i2\Phi)\}$$
$$-Q_0(\omega)Q_0(-\omega)\{1-\exp(i2\Phi)\} \tag{3.120}$$

The expected values of $X(\omega)$ and $|X(\omega)|^2$ are evaluated below first under the assumption that Φ is uniformly distributed between $-a$ and a $(a>0)$.

$$\mathrm{E}\{X(\omega)\}=X_0(\omega)(\sin a/a) \tag{3.121}$$

$$\mathrm{E}\{|X(\omega)|^2\}=|P_0(\omega)|^2+|Q_0(\omega)|^2+2\mathrm{Re}[P_0(\omega)P_0(-\omega)]\{2a/(\sin 2a)\} \tag{3.122}$$

For example, if $a=\pi/2$

$$\mathrm{E}\{X(\omega)\}=2X_0(\omega)/\pi \tag{3.123}$$

$$\mathrm{E}\{|X(\omega)|^2\}=|P_0(\omega)|^2+|Q_0(\omega)|^2 \tag{3.124}$$

and if $a=\pi/4$,

$$\mathrm{E}\{X(\omega)\}=(2\sqrt{2}/\pi)X_0(\omega)\cong X_0(\omega) \tag{3.125}$$

$$\mathrm{E}\{|X(\omega)|^2\}=|P_0(\omega)|^2+|Q_0(\omega)|^2+4\,\mathrm{Re}[P_0(\omega)P_0(-\omega)]/\pi \tag{3.126}$$

If we assume that Φ is Gaussian with zero mean $(\mu=0)$ and standard deviation σ,

$$E\{X(\omega)\}=X_0(\omega)\exp(-\sigma^2/2)=[P_0(\omega)+Q_0(\omega)]\exp(-\sigma^2/2) \tag{3.127}$$

$$E\{|X(\omega)|^2\}=|X_0(\omega)|^2-2\,\mathrm{Re}[P_0(\omega)P_0(-\omega)]\{1-\exp(-2\sigma^2)\} \tag{3.128}$$

As $\sigma\to\infty$, these equations approach the following values:

$$E\{X(\omega)\}=0 \tag{3.129}$$

$$E\{|X(\omega)|^2\}=|P_0(\omega)|^2+|Q_0(\omega)|^2 \tag{3.130}$$

As to the relationship between the autocorrelation function $R_{xx}(t_1, t_2)$ and the generalized spectrum $S_{xx}(\omega_1, \omega_2)$ of the processes of the second kind, Eq. 3.45 is still valid whether we deal with the processes of the first kind or of the second kind. At the same time, the autocorrelation function of the process $x(t)$ can generally be written as

$$R_{xx}(t_1, t_2)=1/(2\pi)^2\int_{-\infty}^{\infty}\int_{-\infty}^{\infty}E[X(\omega_1)X^*(\omega_2)]\times\exp\{i(\omega_1t_1-\omega_2t_2)\}\,d\omega_1\,d\omega_2 \tag{3.131}$$

Therefore, comparing Eqs. 3.131 with 3.45, we obtain

$$S_{xx}(\omega_1, \omega_2)=E[X(\omega_1)X^*(\omega_2)]/(2\pi)^2 \tag{3.132}$$

Substituting Eq. 3.116 into the above, we further obtain

$$S_{xx}(\omega_1,\omega_2)=\Big[X_0(\omega_1)X_0^*(\omega_2)-P_0(\omega_1)P_0(-\omega_2)[1-E\{\exp(-2i\Phi)\}]-Q_0(\omega_1)Q_0(-\omega_2)[1-E\{\exp(2i\Phi)\}]\Big]/(2\pi)^2 \tag{3.133}$$

Hence, if Φ is uniformly distributed between $-a$ and a $(a>0)$,

$$S_{xx}(\omega_1, \omega_2)=\Big[X_0(\omega_1)X_0^*(\omega_2)-P_1(\omega_1)P_0(-\omega_2)\{1-\sin(2a)/(2a)\}-Q_0(\omega_1)Q_0(-\omega_2)\{1-\sin(2a)/(2a)\}\Big]/(2\pi)^2 \tag{3.134}$$

In particular, if $a=m\pi/2$ ($m=$ a positive integer), we can show that

$$S_{xx}(\omega_1, \omega_2)=\Big[P_0(\omega_1)Q_0(-\omega_2)+Q_0(\omega_1)P_0(-\omega_2)\Big]/(2\pi)^2 \tag{3.135}$$

and if $a=\pi/4$,

$$S_{XX}(\omega_1,\omega_2)=\Big[X_0(\omega_1)X_0^*(\omega_2)-\{(\pi-2)/\pi\}\{P_0(\omega_1)P_0(-\omega_2)+Q_0(\omega_1)Q_0(-\omega_2)\}\Big]/(2\pi)^2 \tag{3.136}$$

In the cases where Φ is Gaussian with zero mean ($\mu=0$) and standard deviation σ, we can show that

$$S_{XX}(\omega_1,\omega_2)=\Big[P_0(\omega_1)Q_0(-\omega_2)+Q_0(\omega_1)P_0(-\omega_2)+\{P_0(\omega_1)P_0(-\omega_2)+Q_0(\omega_1)Q_0(-\omega_2)\}\exp(-2\sigma^2)\Big]/(2\pi)^2 \tag{3.137}$$

which, as $\sigma\to\infty$, reduces to

$$S_{XX}(\omega_1,\omega_2)=\Big[P_0(\omega_1)Q_0(-\omega_2)+Q_0(\omega_1)P_0(-\omega_2)\Big]/(2\pi)^2 \tag{3.138}$$

Note that Eq. 3.135 and 3.138 are identical. In all these expressions that appear above, the functions $P_0(\omega)$ and $Q_0(\omega)$ play a major role. We suggest that these functions be evaluated as the Fourier transforms of $p_0(t)$ and $q_0(t)$ as defined in Eqs. 3.103 and 3.102 respectively.

CHAPTER 4 NUMERICAL EXAMPLES AND DISCUSSIONS

4. 1 Introduction

The data-based nonstationary random process models proposed in the preceding chapter are applied to three different sets of observed data. The first is a set of the NS and EW components of the ground acceleration recorded at the time of the Niigata earthquake (1964). Their nonstationary characteristics are conspicuous in temporal variability not only in intensity but also in spectral content. While it is undoubtedly of vital importance to examine the physical significance that such a nonstationarity might suggest (for example, the effect of liquefaction), these records are simulated (without considering physical implications) by the process of the first kind assuming in one case that the two components are independent and in the other that they are statistically dependent. The second set of data consitst of a stretch (360 sec) of a wind pressure record measured at a location on the wall on the leeward side of a building.[33] The record exhibits a considerable asymmetry dominated by negative pressures caused by turbulence in the wake behind the building. The process of the first kind is applied to this record of wind pressure. Finally, the process of the second kind is used to simulate the temporal variations of a normal load factor (in terms of g, acceleration due to gravity) recorded during fighter maneuver actions. The observed data consist of two stretches of actual records of such variations, maneuver load A with a duration of 31.0 sec and maneuver load B with a duration of 69 sec. The process of the second kind is used here to ensure that at the beginning and at the end of a maneuver, the normal load factor is unity since we assume an ideal level flight before and after the maneuver.

4. 2 Earthquake Acceleration

In Figs. 6 and 7, the original record $x_0(t)$, with a duration of 34 sec, the Fourier amplitude $|X_0(\omega)|$ and phase angle $\zeta_0(\omega)$ are plotted respectively for the NS and EW components of the ground acceleration of the 1964 Niigata earthquake. The sharp change in the oscillatory characteristics of these records is apparent at around $t=9$ sec. Fig. 8 plots both the original record $x_0(t)$ of the NS component and its Hilbert transfrom $\hat{x}_0(t)$ in the time interval $[0, T_0]$ with $T_0=34$ sec, while Fig. 9 compares the original record $x_0(t)$ with two sample functions $x^{(1)}(t)$ and $x^{(2)}(t)$ chosen out of the five hundred generated from the data-based nonstationary process of the first kind having a Gaussian Φ with mean $\mu=0$ and standard deviation $\sigma=50\pi$. The standard deviation of 50π is practically large enough to approximate the limiting case of $\sigma\to\infty$. In Fig. 9, we

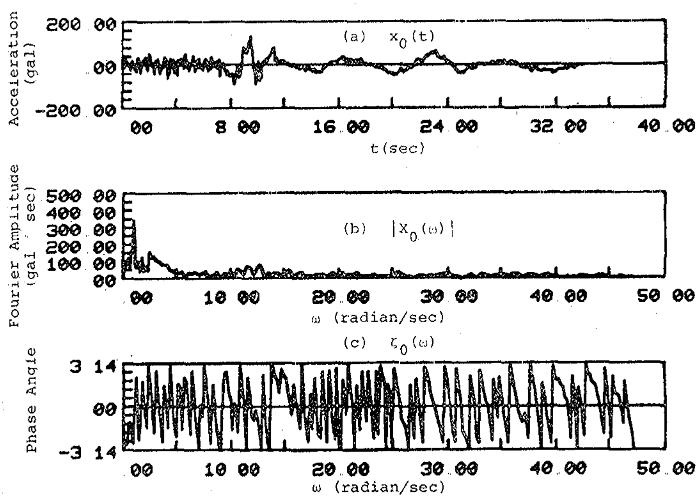

Fig. 6 Original record $x_0(t)$ of NS component of the Niigata earthgquake (1964), Fourier amplitude $|X_0(\omega)|$ and phase angle $\zeta_0(\omega)$.

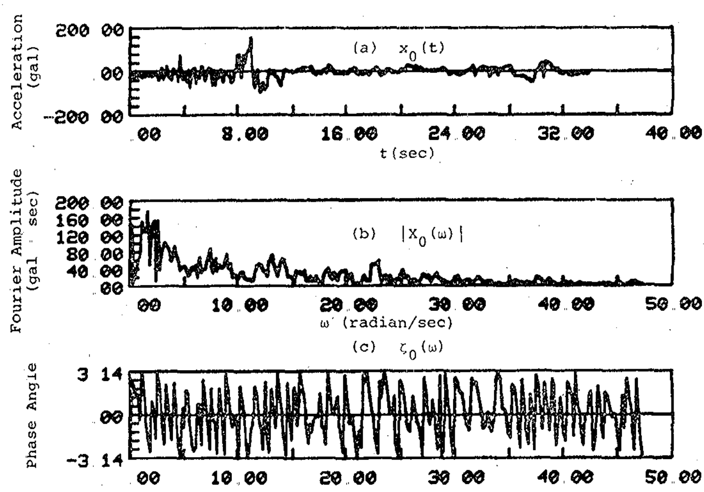

Fig. 7 Original record $x_0(t)$ of EW component of the Niigata earthquake (1964), Fourier amplitude $|X_0(\omega)|$ and phase angle $\zeta_0(\omega)$.

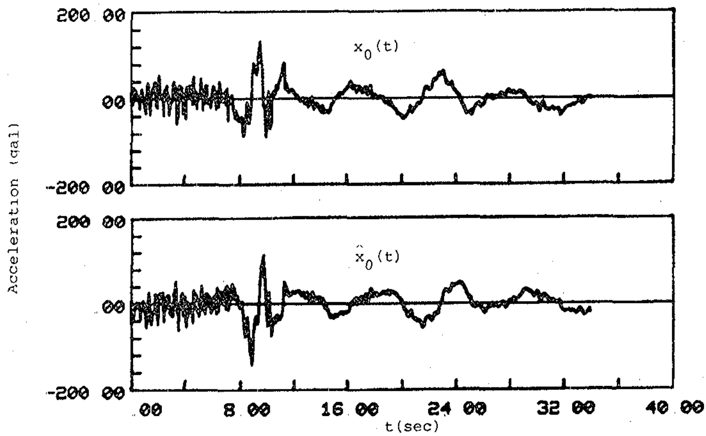

Fig. 8 Original record $x_0(t)$ of NS component of the Niigata earthquake (1964) and its Hilbert transform $\hat{x}_0(t)$.

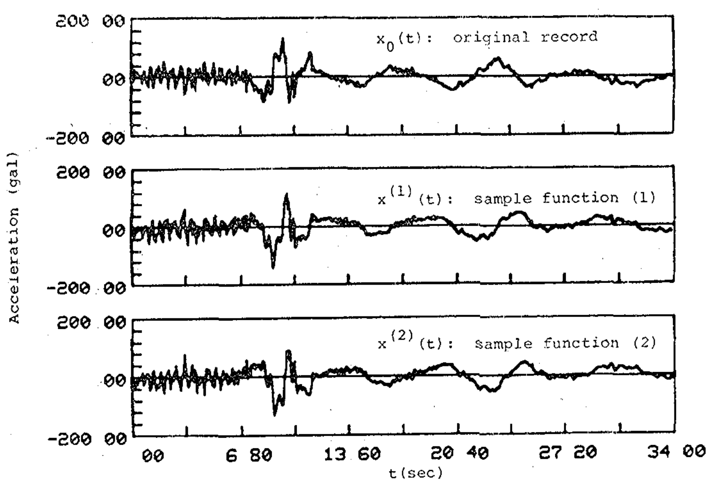

Fig. 9 Original record of NS component of the Niigata earthquake (1964) and sample functions (first kind; Gaussian distribution of Φ with $\mu=0$ and $\sigma=50\pi$).

observe that sample functions faithfully reproduce the temporal variations of the intensity and the frequency content exhibited by the original record. In Fig.10, the Fourier amplitude $|X_0(\omega)|$ of the original record is compared with those of the sample functions, and we observe that these Fourier amplitudes are practically identical.

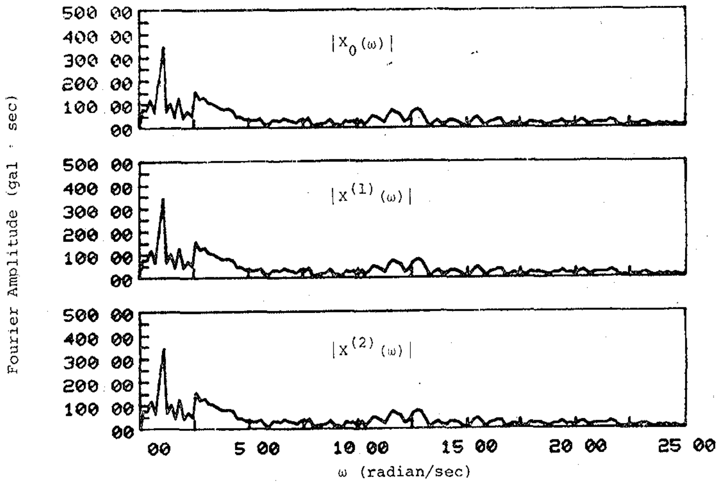

Fig. 10 Fourier amplitudes of original record of NS component of the Niigata earthquake (1964) and of sample functions (first kind; Gaussian distribution of Φ with $\mu=0$ and $\sigma=50\pi$).

While it is not explicitly illustrated in Fig. 8, the Hilbert transform $\hat{x}_0(t)$ of the original record $x_0(t)$ is actually close to zero for the time domains $t\leqq 0$ and $t\geqq T_0$ (=34 sec) due to the fact that the original record fluctuates symmetrically in approximation and rapidly. This is the reason why the sample functions shown in Fig. 9 also have approximately zero initial and terminal values. At the same time, this is responsible for the fact that the Fourier amplitudes of the original record and of the sample functions are all practically identical as shown in Fig. 10, a confirmation of the theoretical assertion that the process of the first kind and its sample function preserve the Fourier amplitude of the original record.

The mean value $E\{x(t)\}$, standard deviation $\sigma_x(t)$, maximum value max $\{x(t)\}$, minimum value min $\{x(t)\}$ and empirical density functions are evaluated by means of the Monte Carlo simulation technique computing the ensemble average on the five hundred sample functions generated.

These statistical quantities, except for the empirical density functions, are shown in Fig. 11 (a)~(d), as functions of time. The empirical density functions at $t=4$ sec, 9 sec and 20 sec are plotted in Fig. 11(e). In Fig. 11, these quantities based on the ensemble averaging coincide so closely when plotted together with the corresponding theoretical values that it is difficult, and therefore no effort is made, to distinguish them except for the density functions.

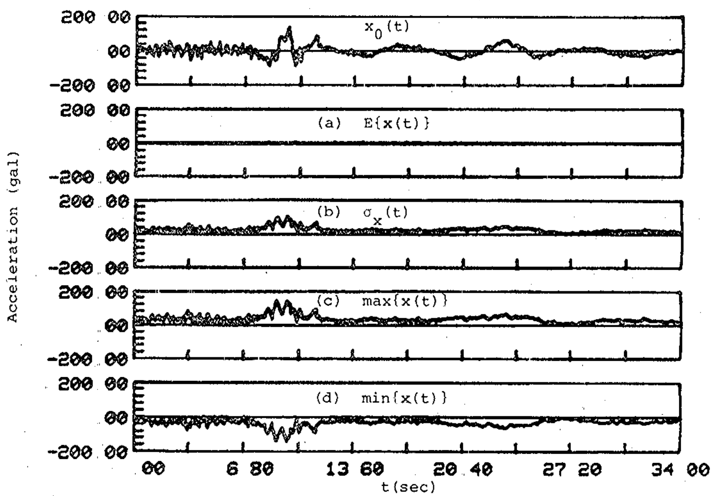

Fig. 11 (a)~(d) Original record $x_0(t)$ of NS component of the Niigata earthquake (1964), mean value, standard deviation, maximum, minimum and empirical density functions (first kind; Gaussian distribution of Φ with $\mu=0$ and $\sigma=50\pi$; sample size=500).

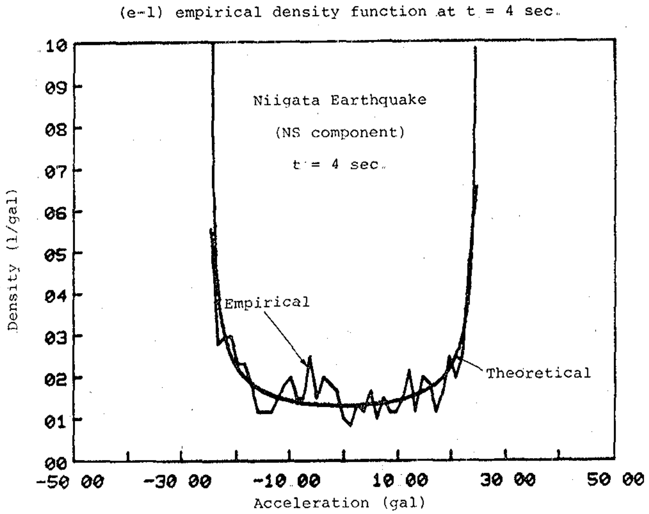

Fig.11 (e)—1 Continued

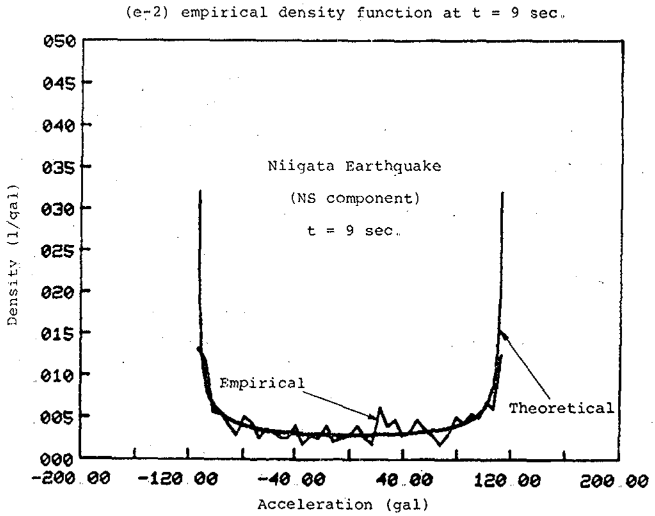

Fig. 11 (e)—2 Continued

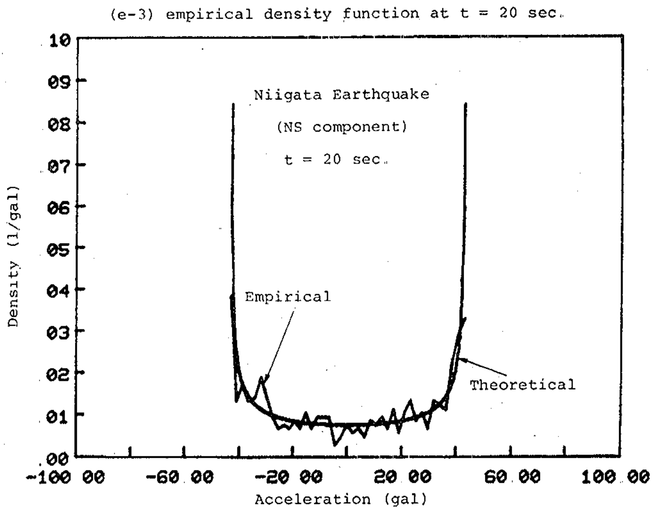

Fig. 11 (e)—3 Continued

Similar results are shown in Figs. 12~15 for the EW component record with the same comments applicable as for the case of the NS component. It is pointed out, however, that the sample functions in this case

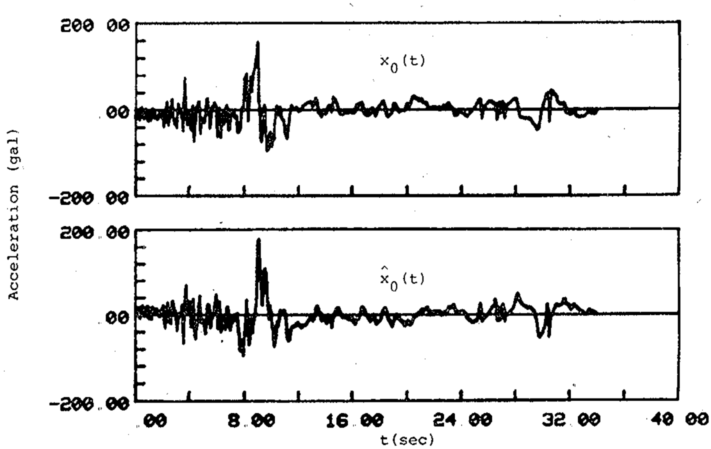

Fig. 12 Original record $x_0(t)$ of EW component of the Niigata earthquake (1964) and its Hilbert transform $\hat{x}_0(t)$.

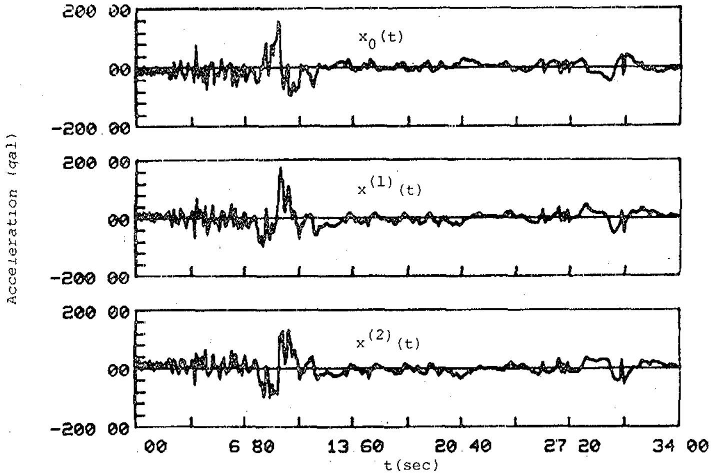

Fig. 13 Original record of EW component of the Niigata earthquake (1964) and sample functions (first kind; Gaussian distribution of Φ with $\mu=0$ and $\sigma=50\pi$).

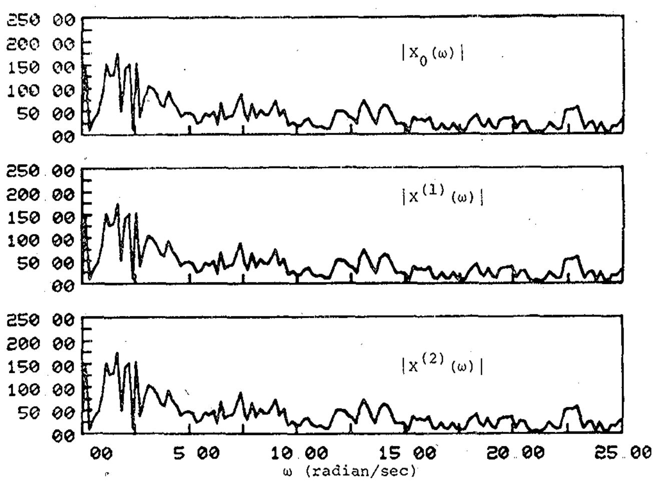

Fig. 14 Fourier amplitudes of original record of EW component of the Niigata earthquake (1964) and of sample functions (first kind; Gaussian distribution of Φ with $\mu=0$ and $\sigma=50\pi$).

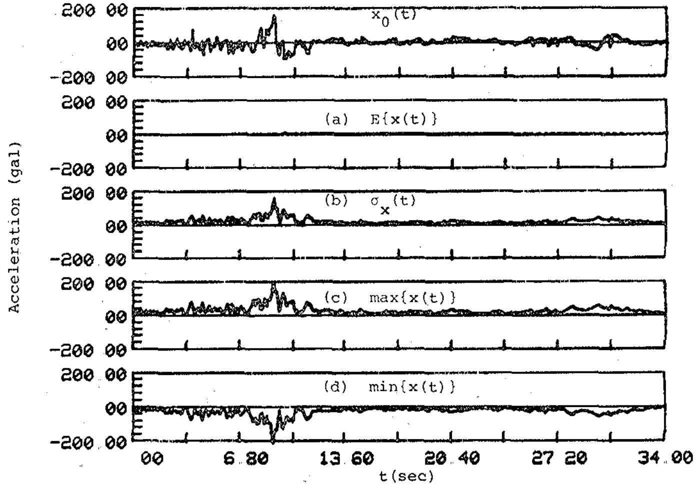

Fig. 15 (a)~(d) Original record $x_0(t)$ of EW component of the Niigata earthquake (1964), mean value, standard deviation, maximum, minimum and empirical density functions (first kind; Gaussian distribution of Φ with $\mu=0$ and $\sigma=50\pi$; sample size=500).

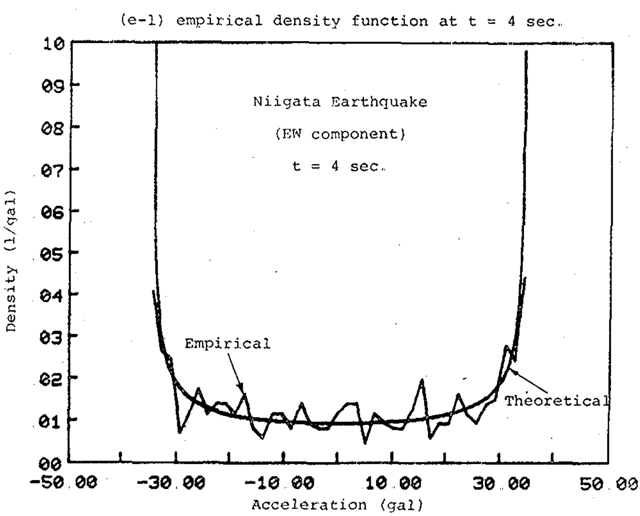

Fig. 15 (e)—1 Continued

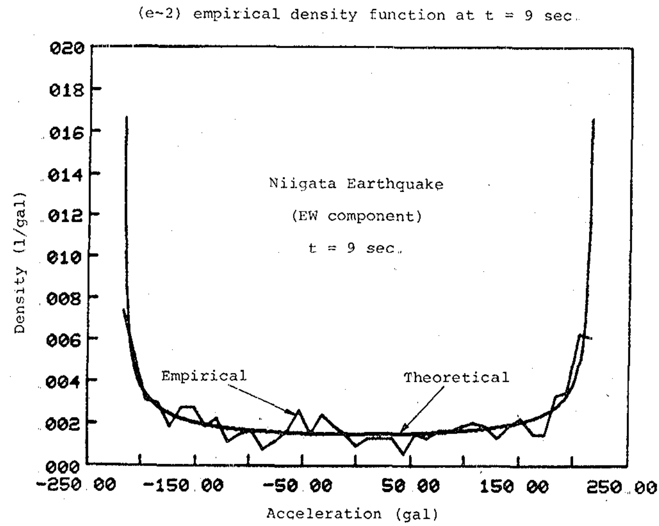

Fig. 15 (e)—2 Continued

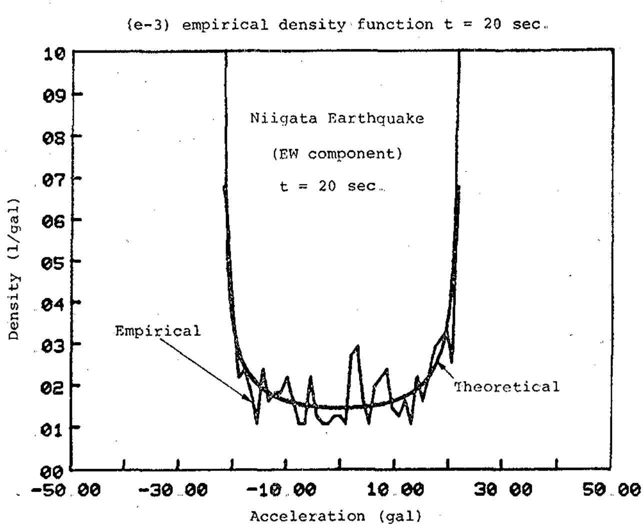

Fig. 15 (e)—3 Continued

are generated under the assumption that the nonstationary process constructed for the EW component is completely independent of the process constructed for the NS component. This implies that two entirely independent sequences of realizations of the random variable Φ are used; one for generating sample functions of the EW component and the other for the NS component.

If we wish to introduce a statistical dependence between the processes $x_1(t)$ and $x_2(t)$ respectively representing the NS and the EW components, they must be assumed to form a bivariate process $\underline{\mathbf{x}}(t)=[x_1(t)\ x_2(t)]^T$ with the component processes $x_1(t)$ and $x_2(t)$ (both of the first kind) constructed with the aid of Eqs. 3.54 and 3.55. In the present study, we further assume that Φ_1 and Φ_2 in Eq. 3.55 are jointly Gaussian with zero mean, identical standard deviation $\sigma=50\pi$ and coefficient of correlation $\rho_{12}=0.999$. Then, the expected values are (see Eq. 3.29)

$$E\{x_1(t)\}=E\{x_2(t)\}\cong 0 \tag{4. 1}$$

the autocorrelation functions are (see Eq. 3.38)

$$R_{x_ix_i}(t_1,\ t_2)\cong \tfrac{1}{2}\{x_{0i}(t_1)x_{0i}(t_2)+\hat{x}_{0i}(t_1)\hat{x}_{0i}(t_2)\} \quad (i=1,2) \tag{4. 2}$$

and the crosscorrelation function is (see Eq. 3.63)

$$R_{x_1x_2}(t_1,\ t_2)\cong \tfrac{1}{2}\{x_{01}(t_1)x_{02}(t_2)+\hat{x}_{01}(t_1)\hat{x}_{02}(t_2)\}\exp(-2.5\pi^2) \tag{4. 3}$$

The original records $x_{01}(t)$ and $x_{02}(t)$ together with their sample functions, two each out of the two sets of five hundred generated, are plotted in Fig. 16. The sample functions of the process $x_1(t)$ shown in Fig 16 are identical with those in Fig. 9 since the same realizations of a Gaussian random variable, referred to as Φ in the case of Fig. 9 and Φ_1 in the case of Fig. 16, are used for both cases. However, this does not apply to the sample functions of the process $x_2(t)$. Indeed, in this case, the sample functions shown in Fig. 16 are constructed using realizations of the random variable Φ_2. These realizations are generated in accordance

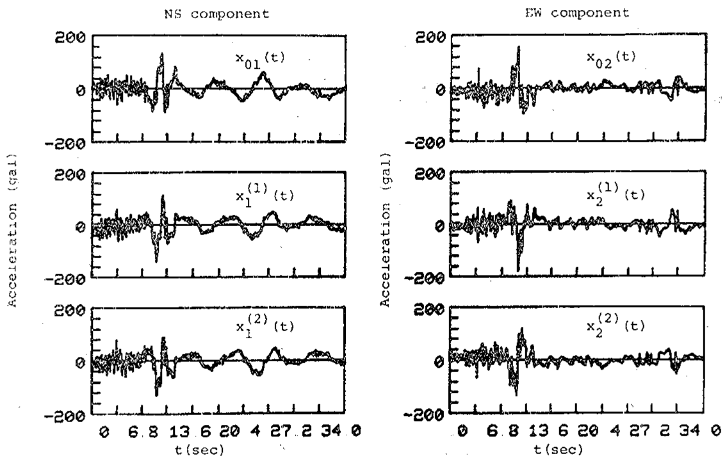

Fig. 16 Acceleration record of the 1964 Niigata earthquake and corresponding artificial acceleration component. (Correlated bivariate process; joint Gaussian distribution for Φ_1 and Φ_2 with $\sigma_{\Phi_1}=\sigma_{\Phi_2}=50\pi$ and $\rho_{\Phi_1\Phi_2}=0.999$). Cross-correlation function $R_{x_1x_2}(t_1,t_2) \cong \frac{1}{2}\{x_{01}(t_1)x_{02}(t_2)+\hat{x}_{01}(t_1)\hat{x}_{02}(t_2)\}\exp(-2.5\pi^2)$

with the "*conditional density function of* Φ_2 *given* Φ_1" which is derived from Eq. 3.62. They are therefore different from those used in the construction of the sample functions in Fig. 13 and hence the two sets of sample functions in Fig. 13 and in Fig. 16 are different. As mentioned earlier, it is the unavailability of such conditional density functions for uniformly distributed Φ's that prevents their use in the multivariate simulation. The Monte Carlo evaluation of the mean value, standard deviation, maximum value, minimum value and empirical density functions of the process $x_2(t)$ statistically dependent upon the process $x_1(t)$ in the manner described above, is performed on the basis of the five hundred sample functions thus generated. As expected, the results are identical with those shown in Fig. 15 since the quantities considered here all depend only on the marginal density function of Φ_2 which in this case is the same density function used independently for generating the results in Fig. 15.

4. 3 Wind Pressure

In Fig 17, the original record $x_0(t)$ of wind pressure, its Fourier amplitude $|X_0(\omega)|$ and phase angle $\zeta_0(\omega)$ are plotted. The Hilbert transform $\hat{x}_0(t)$ of $x_0(t)$ is then computed and plotted in Fig. 18 in the interval

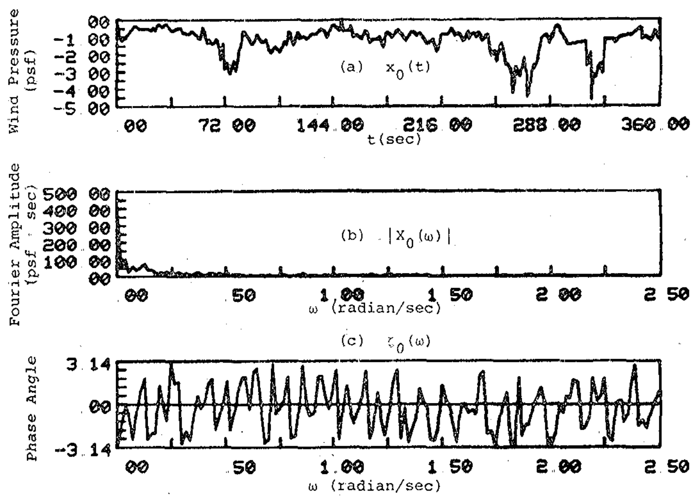

Fig. 17 Original record $x_0(t)$ of wind pressure, Fourier amplitude $|X_0(\omega)|$ and phase angle $\zeta_0(\omega)$.

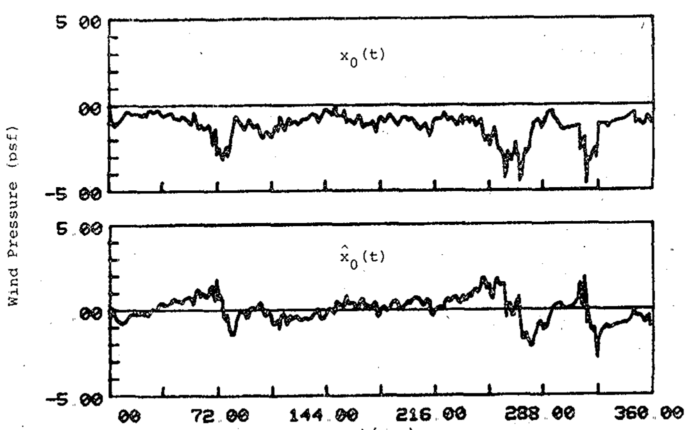

Fig. 18 Original record $x_0(t)$ of wind pressure and its Hilbert transform $\hat{x}_0(t)$.

〔0, T_0〕 (T_0=360 sec) together with the original record $x_0(t)$. While it is not explicitly illustrated in Fig. 18, the Hilbert transform $\hat{x}_0(t)$ of $x_0(t)$ is not necessarily close to zero in the time domains $t \leqq 0$ and $t \geqq T_0$ due to the fact that $x_0(t)$ is dominated by negative pressures. Nevertheless, the data-based nonstationary random process of the first kind is used to simulate the wind pressure, since in this case the condition of zero initial and terminal values does not necessarily have to be strictly observed. The random variable Φ is assumed to distribute uniformly between $-\pi/2$ and $\pi/2$ to simulate the asymmetric nature of the original record (see Eqs. 3.49—3.52). Fig. 19 plots two sample functions (out of the five hundred generated) together with the original record, while Fig. 20, the Fourier amplitudes of these two sample functions as well as of the original. In this case, in spite of the use of data-based process of the first kind, we observe that the Fourier amplitudes of the sample functions

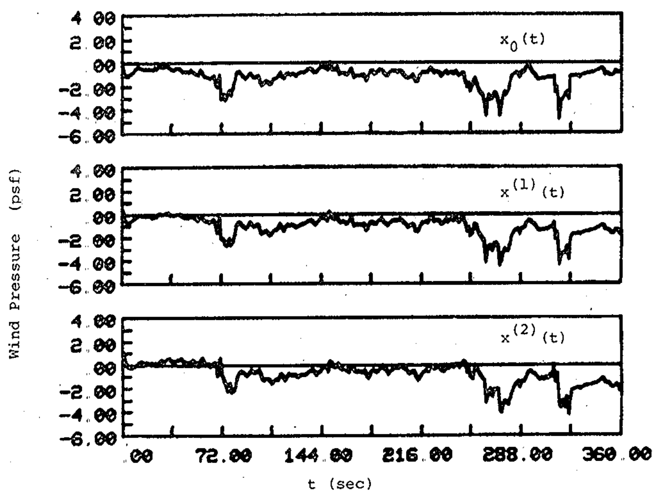

Fig. 19 Original record of wind pressure and sample functions (first kind; uniform distribution of Φ between $-\pi/2$ and $\pi/2$)

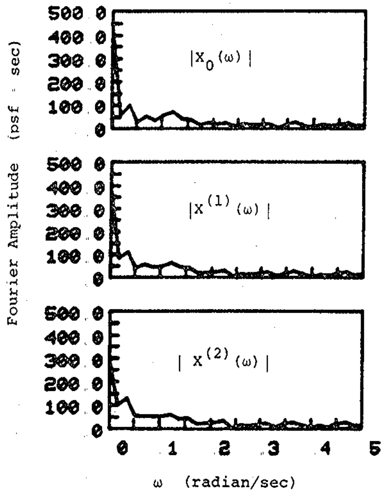

Fig. 20 Fourier amplitudes of original record of wind pressure and of sample functions (first kind; uniform distribution of Φ between $-\pi/2$ and $\pi/2$)

are dissimilar not only to each other but also to that of the original record. This is due to the follwing fact: The Hilbert transform $\hat{x}_0(t)$ and hence $x(t)=x_0(t)\cos\Phi-\hat{x}_0(t)\sin\Phi$ are generally not close to zero but have no insignificant values outside the interval $[0, T_0]$. Therefore, if we construct sample functions, as we do here, by extracting that portion of $x(t)$ which exsends only over the interval $[0, T_0]$ and evaluate its Fourier amplitude, we then find that the Fourier amplitude depends on each sample function and is usually smaller than $|X_0(\omega)|$ corresponding to the original (this is consistent with the Parseval theorem)(※8). The Monte Carlo

(*8) Let $F_1(\omega)$ and $F_2(\omega)$ be the Fourier transforms of $f_1(t)$ and $f_2(t)$, respectively. Then the Parseval theorem states that

$$\int_{-\infty}^{\infty} f_1(t) f_2(t)\, dt = \frac{1}{2\pi}\int_{-\infty}^{\infty} F_1(-\omega) F_2(\omega)\, d\omega$$

If $f_1(t)=f_2(t)=f(t)$, with $F(\omega)$ being its Fourier transform and $f(t)$ being a real function of t,

$$\int_{-\infty}^{\infty} \{f(t)\}^2\, dt = \frac{1}{2\pi}\int_{-\infty}^{\infty} F(-\omega)F(\omega)\,d\omega = \frac{1}{2\pi}\int_{-\infty}^{\infty} |F(\omega)|^2\, d\omega$$

since for a real function $f(t)$ we have $F(-\omega)=F^*(\omega)$.

evaluation of the mean value, standard deviation, maximum value and minimum value are plotted as functions of time in Fig. 21(a)~(d) while the empirical density function of $x(t)$ at $t=180$ sec. is in Fig. 21 (e).

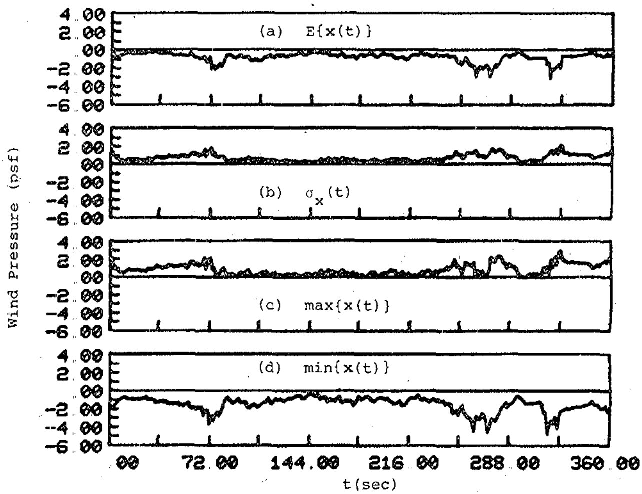

Fig. 21 (a)~(d) Mean value, standard deviation, maximum, minimum and empirical density function of the simulated wind pressure process (first kind; uniform distribution of Φ between $-\pi/2$ and $\pi/2$; sample size=500).

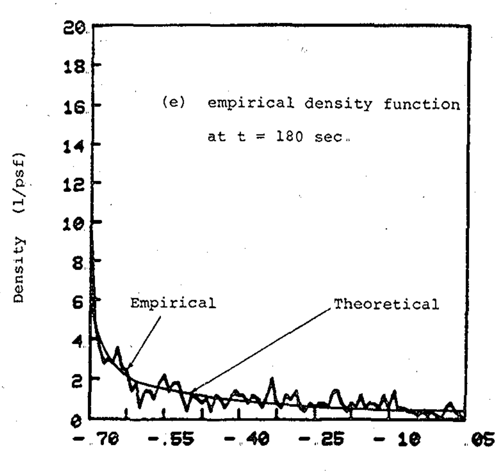

Fig. 21(e) Continued

The results in Fig. 21 (a)～(d) also represent the theoretical evaluation of the same quantities since the Monte Carlo and theoretical evaluations have been found to be in almost perfect agreement.

4. 4 Maneuver Loads

Two sets (cases A and B) of temporal variations in the normal load factor observed during fighter maneuver actions are considered. These temporal variations, their Fourier amplitudes and phase angles are plotted in Figs. 22 and 23 respectively for maneuver A (duration $T_0=31$ sec) and maneuver B (duration $T_0=69$ sec). Both maneuver loads are dominated by positive values and hence their Hilbert transforms are not close to zero at $t=0$ and $t=T_0$ even in approximation. This implies that the use of the data-based process of the first kind will not produce desired sample functions which begin and end with zero values. Therefore, the data-based process of the second kind is used to simulate these maneuver loads. In both cases, the random variable Φ is assumed to be uniformly

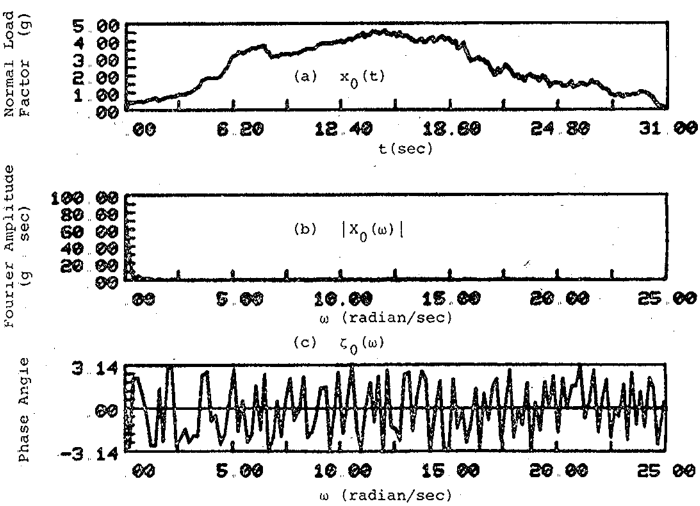

Fig. 22 Original record $x_0(t)$ of maneuver load A, Fourier amplitude $|X_0(\omega)|$ and phase angle $\zeta_0(\omega)$.

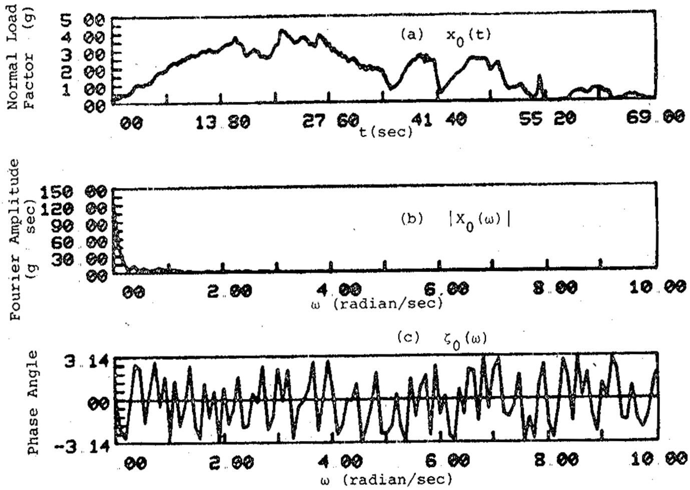

Fig. 23 Original record $x_0(t)$ of maneuver load B, Fourier amplitude $|X_0(\omega)|$ and phase angle $\zeta_0(\omega)$.

distributed between $-\pi/2$ and $\pi/2$.

Dealing first with maneuver load A, the symmetric-periodic extension $z_0(t)$ of the original record $x_0(t)$ and the Hilbert transform $\hat{z}_0(t)$ of $z_0(t)$

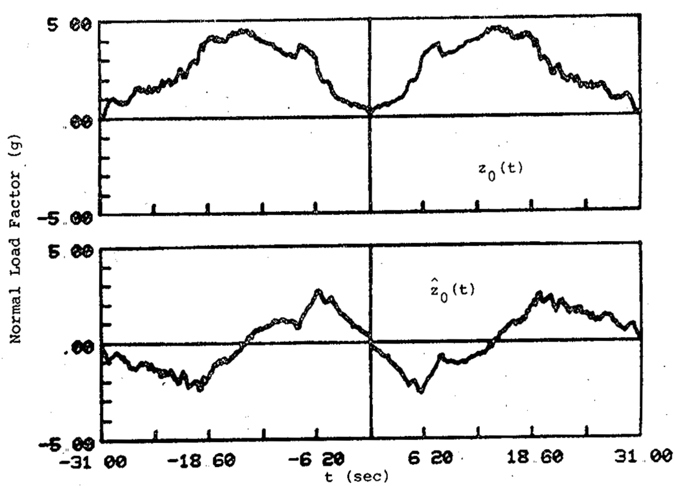

Fig. 24 Symmetric-periodic extension $z_0(t)$ of manuever load A and its Hilbert transform $\hat{z}_0(t)$

are plotted in Fig. 24. In Fig. 25, the Fourier amplitude $|X_0(\omega)|$ of $x_0(t)$ is plotted together with the quantities $\{|P_0(\omega)|^2+|Q_0(\omega)|^2\}^{1/2}$, $|P_0(\omega)|$ and $|Q_0(\omega)|$. The quantity $\{|P_0(\omega)|^2+|Q_0(\omega)|^2\}^{1/2}$ is of particular importance since this is equal to $[E\{|X(\omega)|^2\}]^{1/2}$ under the current assumption of Φ and is to be compared with $|X_0(\omega)|$. Indeed, if the difference between $|X_0(\omega)|$ and $\{|P_0(\omega)|^2+|Q_0(\omega)|^2\}^{1/2}=[E\{|X(\omega)|^2\}]^{1/2}$ is small, it indicates that the simulated process (of the second kind), on the average with a small alteration, has preserved the Fourier amplitude of the original record while ensuring zero initial and terminal conditions. We observe in Fig. 25 some reduction in the value of $\{|P_0(\omega)|^2+|Q_0(\omega)|^2\}^{1/2}$ for small values of ω. This is consistent with a further observation in Fig. 26 that all of the three sample functions shown therein exhibit generally smaller normal load factors than the original record. This trend exists for most of the five hundred sample functions generated and is one of the characteristics of the process of the second kind. Fig. 27 plots the Fourier amplitudes of the original record and of the sample functions shown in Fig. 26. The Monte Carlo evaluation of the mean value, standard deviation, maximum value and minimum value are plotted as functions of time in Fig. 28 (a)～(d) while the empirical density function at $t=15.5$ sec is plotted in Fig. 28 (e) on the basis of the five hundred sample functions. Fig. 28 (a)～(d) also serve as the plot

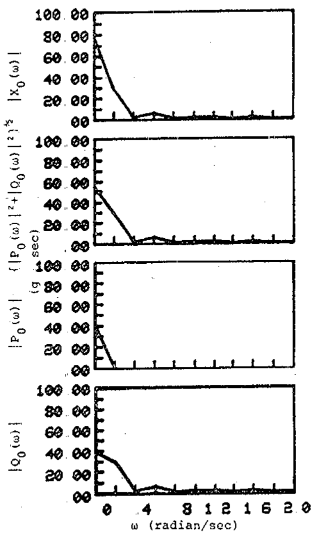

Fig. 25 $|X_0(\omega)|$, $\{|P_0(\omega)|^2+|Q_0(\omega)|^2\}^{1/2}$, $|P_0(\omega)|$ and $|Q_0(\omega)|$ for maneuver load A.

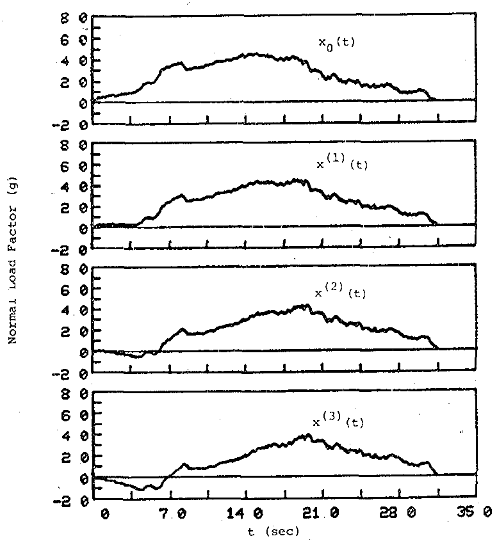

Fig. 26 Original record of maneuver load A and sample functions (second kind; uniform distribution of Φ between $-\pi/2$ and $\pi/2$)

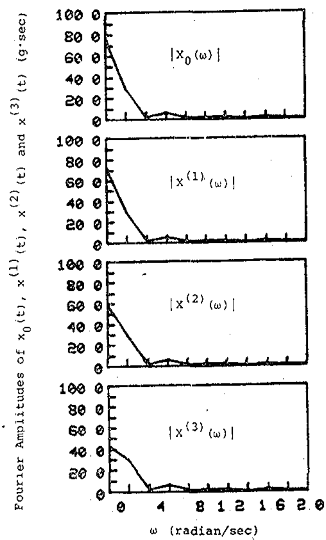

Fig. 27 Fourier amplitudes of original record of maneuver load A and of sample functions (second kind; uniform distribution of Φ between $-\pi/2$ and $\pi/2$)

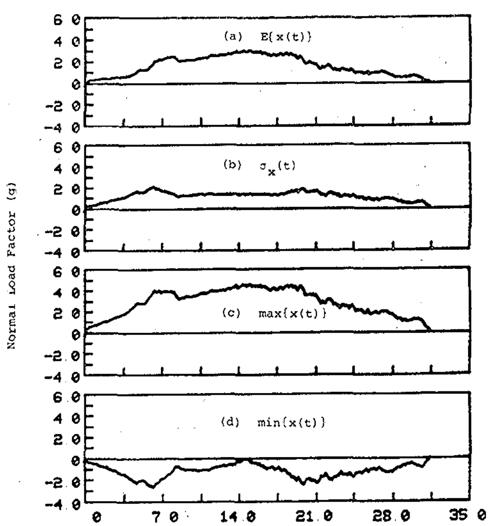

Fig. 28 (a)~(d)
Mean value, standard deviation, maximum, minimum and empirical density function of the simulated maneuver load A (second kind; uniform distribution of Φ between $-\pi/2$ and $\pi/2$; sample size=500).

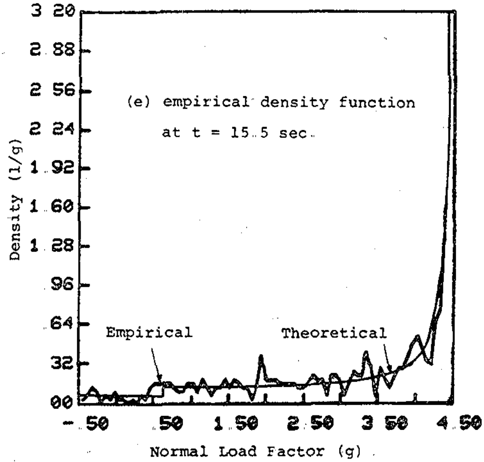

Fig. 28 (e) Continued

of the theoretical values for the corresponding quantities for the same reasons as repeated above.

Similar results for maneuver load B are obtained in Figs. 29~33 with the same comments applicable as for the case of maneuver load A.

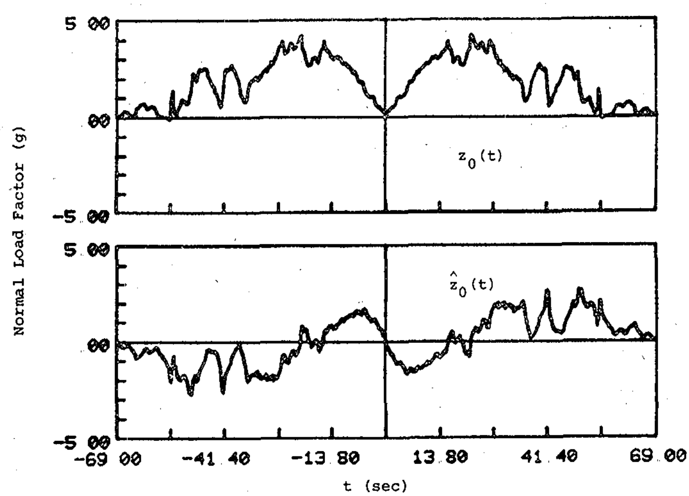

Fig. 29 Symmetric-periodic extension $z_0(t)$ of maneuver load B and its Hilbert transform $\hat{z}_0(t)$

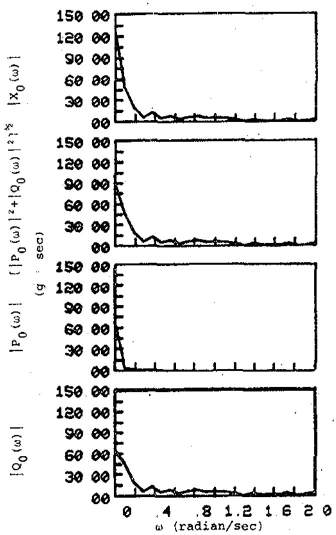

Fig. 30 $|X_0(\omega)|$, $\{|P_0(\omega)|^2+|Q_0(\omega)|^2\}^{1/2}$, $|P_0(\omega)|$ and $|Q_0(\omega)|$ for maneuver load B.

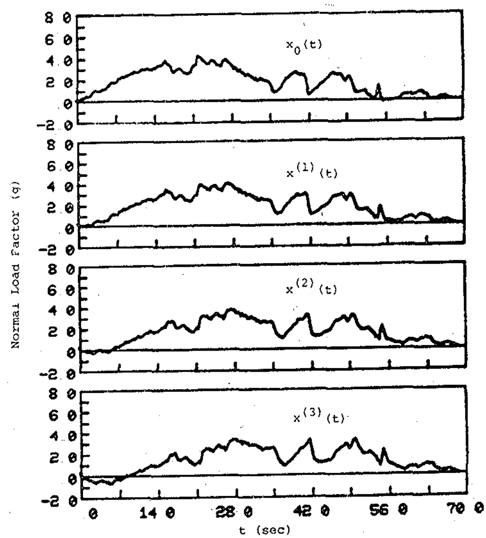

Fig. 31 Original record of maneuver load B and sample functions (second kind; uniform distribution of Φ between $-\pi/2$ and $\pi/2$)

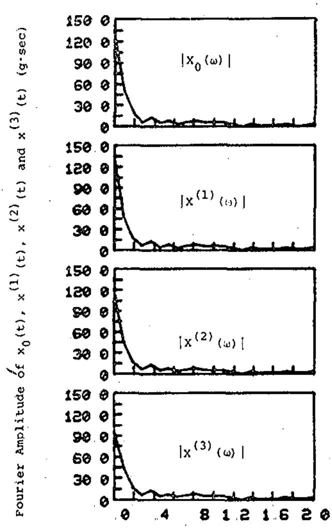

Fig. 32 Fourier amplitudes of original record of maneuver load B and of sample functions (second kind; uniform distribution of Φ between $-\pi/2$ and $\pi/2$)

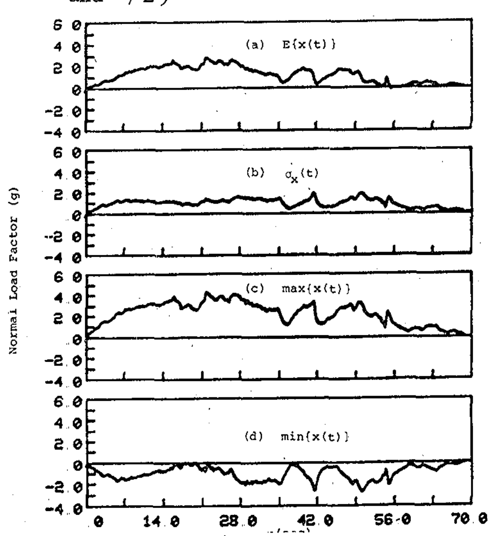

Fig. 33 (a)~(d) Mean value, standard deviation, maximum, minimum and empirical density function of the simulated maneuver load B (second kind; uniform distributlon of Φ between $-\pi/2$ and $\pi/2$, sampe size=500).

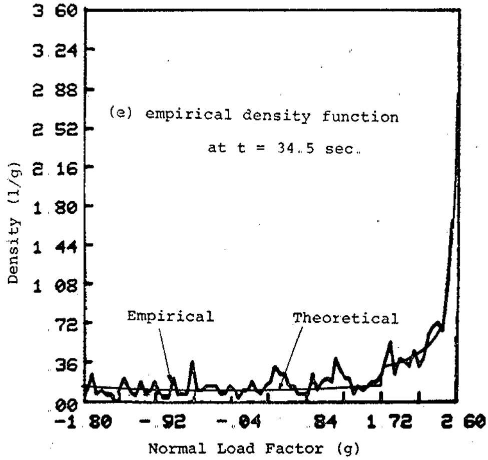

Fig.33 (e) Continued

CHAPTER 5 CONCLUSION

As one of the nonstationary random process models to be characterized primarily in terms of the frequency domain behaviors, the data-based non-stationary random process models of the first and second kind have been introduced.

The model can be written as the inversion of the Fourier transform of the original record (the first kind) or of its symmetric-periodic extension (the second kind) with the phase angle shifted by a random amount Φ. It is this shift that introduces the randomness into the model.

The processes of the first kind preserve, in principle, the Fourier amplitude of the original record while those of the second kind do so only in approximation. The latter however strictly observe the zero initial and terminal conditions if the original record does. The data-based multi-variate process model of the first kind is also introduced.

The construction of the data-based process model is a straightforward task requiring only the Fourier transform of the original record (or its extension) or equivalently its Hilbert transform: No theoretical or numerical finesse needs to be exercised in the construction of the model, thus obviating the necessity of the engineer analyzing the data, to be an expert in random process theory and data analysis.

The following quantities associated with the data-based nonstationary random process are theoretically evaluated: the mean value, standard deviation, maximum value, minimum value, probability density function, autocorrelation function, generalized spectrum, crosscorrelation function and cross-spectral density function (in multi-variate situation).

The model lends itself to a tractable implementation of Monte Carlo analyses since it can generate sample functions with ease.[34] The validity of such Monte Carlo analyses can be checked by comparing the Monte Carlo estimation of some of the quantities just mentioned with their corresponding theoretical values.

Three sets of observed data are used for numerical examples. The NS and EW components of the ground acceleration of the 1964 Niigata earthquake are simulated by the processes of the first kind; in one case as two independent processes (with independent Φ's) and in the other as a bivariate process with a correlation between the component processes (with dependent Φ's). In both cases, we assume that the random variable Φ is Gaussian obtaining the simulated processes of symmetric distribution. The process of the first kind is also used to simulate a stretch of a wind pressure record with Φ distributed uniformly between $-\pi/2$ and $\pi/2$ to emphasize its asymmetric behaviors. Finally, two records of the acceleration representing the normal load factor for a fighter aircraft during its maneuver actions are analyzed and simulated by the process of the second kind with Φ distributed uniformly between $-\pi/2$ and $\pi/2$ again to reproduce the asymmetric characteristics of the records. A set of five hundred sample functions are generated for each of the example cases mentioned above for the purpose of a Monte Carlo verification of the theoretically evaluated mean value, standard deviation, etc. The agreement between the Monte Carlo and theoretical results has been found to be practically perfect.

ACKNOWLEDGEMENT: This work was supported by the National Science Foundation jointly under NSF-ENG-76-12257 and NSF-PFR-78-15049.

REFERENCES

(1) Shinozuka, M., Ishikawa, H., and Mitsuma, H., "Development of A Data-Based Artificial Acceleration Model," Proc. of the Fifth National Meeting of UCEER (University Council for Earthquake Engineering Research), at MIT, Boston, Mass., U. S. A., June, 1978, pp. 59—61.

(2) Shinozuka, M., Ishikawa, H., and Mitsuma, H., "Data-Based Nonstationary Random Processes," Proc. of Specialty Conference on Probabilistic Mechanics and Structural Reliability, ASCE, (1979) Tucson, Az., U. S. A., pp. 39—43.

(3) Parzen, E., "*Stochatic Processes*" Holden-Day, Inc., San Francisco, 1964, pp. 144—157.

(4) Rice, S. O., "Mathematical Analysis of Random Noise," in "*Selected Papers on Noise and Stochastic Processes*" edited by N. Wax, Dover Publications, Inc., New York, 1954, p. 180.

(5) Lin, Y. K., "*Probabilistic Theory of Structural Dynamics*," McGraw-Hill Book Company, New York, 1967, pp. 94—95 and pp. 132—142.

(6) Shinozuka, M. and Sato, Y., "Simulation of Nonstationary Random Process," EMD Journal, ASCE, Vol. 93, No. EM1, February 1967, pp. 11—40.

(7) Bendat, J. S., Enochson, L. D., Klein, G.H. and Piersol, A. G., "Advanced Concepts of Stochastic Processes and Statistics for Flight Vehicle Vibration Estimation and Measurement," ASD-TDR-62—973, Thompson Ramo Woolbridge Inc., December, 1962, pp. 5-1 — 5-19.

(8) Caughey, T. K., "Nonstationary Random Inputs and Responses," in "*Random Vibration*," Vol. 2, edited by Crandall, S. H., MIT Press, 1963, pp. 66—84.

(9) Papoulis, A., "*Probability, Random Variables and Stochastic Processes*," McGraw-Hill Book Company, Inc., New York, 1965, pp. 430—452.

(10) Roberts, J.B., "On the Harmonic Analysis of Evolutionary Random Vibration," Journal of Sound and Vibration, 2 (3), 1965, pp. 336—352.

(11) Page, C. H., "Instantaneous Power Spectra," Journal of Applied Physics, Vol. 23, No. 1, January, 1952, pp. 103—106.

(12) Liu, S. -C., "Time-Varying Spectra and Linear Transformation," The Bell System Technical Journal, Vol. 50, No. 7, September, 1971, pp. 2365—2374.

(13) Liu, S. -C., "An Approach to Time-Varying Spectral Analysis," EMD Journal, ASCE, Vol. 98, No. EM 1, February, 1972, pp. 243—253.

(14) Ville, J., "Théorie et Applications de la Notion de Signal Analytique," Cabies et Trans., 2, 1948, pp. 61—74.

(15) Bendat, J. S. and Piersol, A. G., "*Measurement and Analysis of Random Data*," John Wiley & Sons, Inc., New York, 1966, pp. 364—365.

(16) Mark, W. D., "Spectral Analysis of the Convolution and Filtering of Non-stationary Stochastic Processes, "Journal of Sound and Vibration, 11 (1), 1970, pp. 19—63.

(17) Mark, W. D., "Power Spectral Representation of Nonstationary Random Processes Defined Over Semi-infinite Intervals," Journal of the Acoustical Society of America, Vol. 59, No. 5, May, 1976, pp. 1184—1194.

(18) Priestley, M.B., "Evolutionary Spectra and Non-stationary Processes," Journal of the Royal Statistical Society, B 27, No. 2, 1965, pp. 204—237.

(19) Priestley, M. B., "Design Relations for Non-stationary Processes," Journal of the Royal Statistical Society, B 28, No. 1, 1966, pp. 228—240.

(20) Priestley, M. B., "Power Spectral Analysis of Non-stationary Random Processes," Journal of Sound and Vibration, 6 (1), 1967, pp. 86-97.

(21) Priestly, M. B., "Some Notes on the Physical Interpretation of Spectra of Non-stationary Stochastic Processes," Journal of Sound and Vibration, 17(1), 1971, pp. 51—54.

(22) Hammond, J. K., "On the Response of Single and Multidegree of Freedom Systems to Non-stationary Random Excitations," Journal of Sound and Vibration, 7 (3), 1968, pp. 393—416.

(23) Shinozuka, M., "Random Processes with Evolutionary Power," EMD Journal, ASCE, Vol. 96, No. EM4, August, 1970, pp. 543—545.

(24) Shinozuka, M., "Digital Simulation of Random Processes in Engineering Mechanics With the Aid of FFT Technique," in "*Stochastic Problems in Me-*

chanics," edited by Ariaratnam, S. T. and Leipholz, H. E., University of Waterloo Press, 1974, pp. 277—286.

(25) Shinozuka, M, "Time and Space Domain Analysis in the Structural Reliability Assessment, "Proceedings of the Second International Conference on Structural Safety and Reliability, Munich, Germany, September 19—21, 1977, pp. 9—28.

(26) Howell, L. J. and Lin, Y. K., "Response of Flight Vehicles to Nonstationary Atmospheric Turbulence," AIAA Journal, Vol. 9, No. 11, November, 1971, pp. 2201—2207.

(27) Yang, J. -N., "Simulation of Random Envelope Processes," Journal of Sound and Vibration, 21 (1), 1972, pp. 73—85.

(28) Kameda, H., "Evolutionary Spectra of Seismogram by Multifilter," EMD Journal, ASCE, Vol. 101, No. EM 6, December, 1975, pp. 787—801.

(29) Ishikawa, H., "Reliability Analyses of Fatigue Lives of Machines and Structures under Service Loads; Part (VI) Statistical Properties of Service Loads," Journal of JSMS, Vol. 24, No. 264, 1975, pp. 914—924.

(30) Ishikawa, H. and Kimura, H., "Application of Stochastic Process Theory to Fatigue Life Estimation under Service Loading," the Kagawa University Economic Review, Vol. 52, No. 1・2, 1979, pp. 96—183.

(31) Papoulis, A., "*The Fourier Integral and Its Applications*," McGrow-Hill Book Company Inc., New York, 1962, p. 277.

(32) Cramér, H. and Leadbetter, M. R., "*Stationary and Related Stochastic Processes*," John Wiley & Sons, Inc., New York, 1967, p. 248.

(33) Dalgliesh, W. A., "Statistical Treatment of Peak Gusts on Cladding," Journal of the Structural Division, ASCE, ST9, Vol. 97, 1971, qp. 2173—2187.

(34) Vaicaitis, R., Ishikawa, H., and Shinozuka, M., "Dynamic Response and Failure of Window Panes," Proc. of Specialty Conference on Probabilistic Mechanics and Structural Reliability, ASCE, (1979), Tucson, Az., USA, pp. 265—269.